ICRA2009

2009 IEEE International Conference
on Robotics and Automation
Kobe, Japan, May 12-17, 2009

Control issues in the micro/nano-world

Full-day Workshop, May 17 2009

Micky Rakotondrabe
John T. Wen
Philippe Lutz

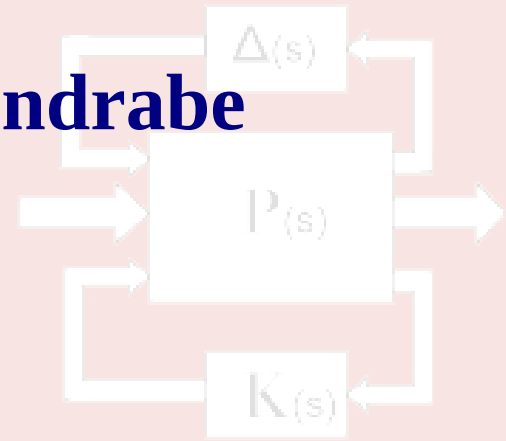

Workshop Contents

Introduction

During the last decade, the need of systems with micro/nanometers accuracy and fast dynamics has been growing rapidly. Such systems occur in applications including 1) micromanipulation of biological cells, 2) micrassembly of MEMS/MOEMS, 3) micro/nanosensors for environmental monitoring, 4) nanometer resolution imaging and metrology (AFM and SEM). The scale and requirement of such systems present a number of challenges to the control system design that will be addressed in this workshop.

Working in the micro/nano-world involves displacements from nanometers to tens of microns. Because of this precision requirement, environmental conditions such as temperature, humidity, vibration, could generate noise and disturbance that are in the same range as the displacements of interest.

The so-called smart materials, e.g., piezoceramics, magnetostrictive, shape memory, electro-active polymer, have been used for actuation or sensing in the micro/nano-world. They allow high resolution positioning as compared to hinges based systems. However, these materials exhibit hysteresis nonlinearity, and in the case of piezoelectric materials, drifts (called creep) in response to constant inputs In the case of oscillating micro/nano-structures (cantilever, tube), these nonlinearities and vibrations strongly decrease their performances.

Many MEMS and NEMS applications involve gripping, feeding, or sorting, operations, where sensor feedback is necessary for their execution. Sensors that are readily available, e.g., interferometer, triangulation laser, and machine vision, are bulky and expensive. Sensors that are compact in size and convenient for packaging, e.g., strain gage, piezoceramic charge sensor, etc., have limited performance or robustness. To account for these difficulties, new control oriented techniques are emerging, such as[d the combination of two or more 'packageable' sensors , the use of feedforward control technique which does not require sensors, and the use of robust controllers which account the sensor characteristics.

The aim of this workshop is to provide a forum for specialists to present and overview the different approaches of control system design for the micro/nano-world and to initiate collaborations and joint projects.

Micky Rakotondrabe[1],
John T. Wen[2]
and Philippe Lutz[1].

[1]Automatic Control and Micro-Mechatronic Systems Department (AS2M),
FEMTO-st Institute,
UMR CNRS 6174 - UFC / ENSMM / UTBM
24, rue Alain Savary
25000 Besançon – FRANCE

mrakoton@femto-st.fr
plutz@femto-st.fr

[2]Department of Electrical, Computer, and Systems Eng,
Center for Automation Technologies and Systems (CATS),
Rensselaer Polytechnic Institute,
CII 8015, 110 8th St.,
Troy, NY 12180-3590

wenj@rpi.edu

Main aspects of the control issues in the micro/nano-world

Micky Rakotondrabe, *Member, IEEE* and Philippe Lutz, *Member, IEEE*

***Abstract*— In this paper, we present a summary of the main properties and difficulties when performing the characterization, the measurement, the identification and the control of systems dedicated to the micro/nano-world.**

I. Introduction

Microworld (resp. nanoworld) is exclusively the world of objects, structures and products of which the volume is cubic micrometre (resp. cubic nanometre). Well known examples of them are the so called NEMS or MEMS/MOEMS (Nano or Micro Opto Electro Mechanical Systems). The MEMS market was forecasted to grow significantly between 2005 and 2015. Their main principal applications are pressure and inertial sensors, read/write heads for hard disks, optical displays, microspectrometers and adaptive peacemakers [1]. The need of manipulation and characterization of biological objects in medical application leads the researchers in the fields of MEMS to take it in interest [2][3][4].

To characterize, measure, control and manipulate objects in the microworld, problems that are unusual in conventional tasks arise. These problems are due to the specific complexity and characteristics of the microworld (adhesion forces), the fact that this complexity is not yet well mastered, and the lack of convenient technology and sensors that would give the same peformances for microworld than recent technology and sensors give for macroworld.

This paper presents the different characteristics when performing the characterization, the measurement, the identification and the control of systems dedicated to the micro/nano-world.. The aim is to rapidly situate in this domain the readers that are novice and to remind the problematic for others.

II. The need of active materials

Positioning or manipulating a micro-object requires a very high accuracy, micrometric or submicrometric. To reach such a performance, instead of using hinges, one uses active materials to develop microactuators, microrobots, micromanipulators and microsystems (Fig. 1-a). The main reason is that imprecision due to mechanical clearances are minimized. In addition, it makes possible to have one bulk structures that are easily embarkable. As example, Shape Memory Allow (thermal and magnetic SMA) [5][6][7], Electrostatic [8], Piezoelectric [9][10] and thermal bimorph [11] materials have been successfully used to design microactuators and microrobots. Fig. 1-b shows an example of a microgripper based on piezoelectric material.

FEMTO-st Institute,
UMR CNRS-6174 / UFC / ENSMM / UTBM
Automatic Control and Micro-Mechatronic Systems department (AS2M department)
25000 Besançon - France
{mrakoton, plutz}@femto-st.fr

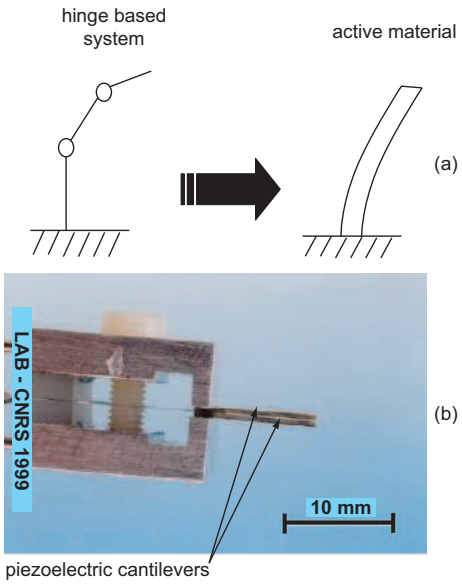

Fig. 1. (a): hinges based systems are replaced by active materials based systems. (b): a piezoelectric microgripper made up of two piezocantilevers [9].

III. The need of new motion principles

In order to reach the necessary accuracy required in the microworld applications, active materials are used. Moreover, some of these materials -such as piezoelectric materials- offer a large bandwidth. Because of the limited deformation of the materials, the range of displacement of the microactuators and microrobots are also limited. In some applications, like microassembly tasks, long displacements are sometimes required. For these cases, new principles of displacements based on active materials microactuators have been proposed: step-by-step motion principles. Step-by-step micropositioning systems can be ranked into two: those based on the inch-worm motion principle and those based on the inertial-drive motion principle. For both, active materials are still used and very high resolutions can be obtained.

Inch-worm systems usually use at least three active material based microactuators. In the example of Fig. 2,

the three microactuators A, B and C works in expansion/contraction inside a tube-shaped support. A step Δx can be got by six successive states of the whole system. Each of these states is obtained by suitably supplying the different actuators (see Fig. 2). By repeating the sequence, the micropositioning system performs a long displacement.

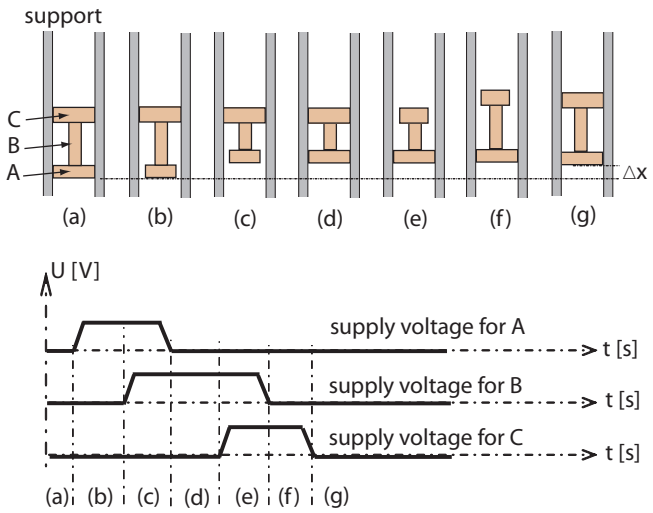

Fig. 2. The inch-worm motion principle.

Inertial-drive motion principle generally uses two techniques: the stick-slip and the impact-drive techniques [12]. For both, a saw-tooth voltage input is used. However, the difference lies in the mass in contact with the support. For stick-slip systems, this mass is smaller than the mass to be moved (Fig. 2-a) while it is greater for impact drive systems (Fig. 2-b). The principle is similar for the two techniques. Fig. 2-c presents a stick-slip system made up of the body to be moved and two microactuators. To obtain a step Δx, a low slope voltage is first applyed, afterwards the amplitude is brusquely reset to zero. When repeating the sequence, the system will move setp-by-step. Fig. 4 pictures a stick-slip micropositioning system that can perform linear and angular motions. Its resolution (step) ranges between $70nm$ and $200nm$ while its speed can reach $2mm/s$ in the linear motion [13].

Because of the step-by-step behavior of inch-worm and inertial-drive systems, it is possible to control them by two modes.

- **The coarse positioning**: the system, which moves step-by-step, is controlled to cover a large range of displacement [14].
- **The fine positioning**: the system only works within a step in order to achieve a very high accuracy. Classical controllers can be used for that [13].

It is also possible to combine the two modes of motion by using only one synthesized controller [15][16][17].

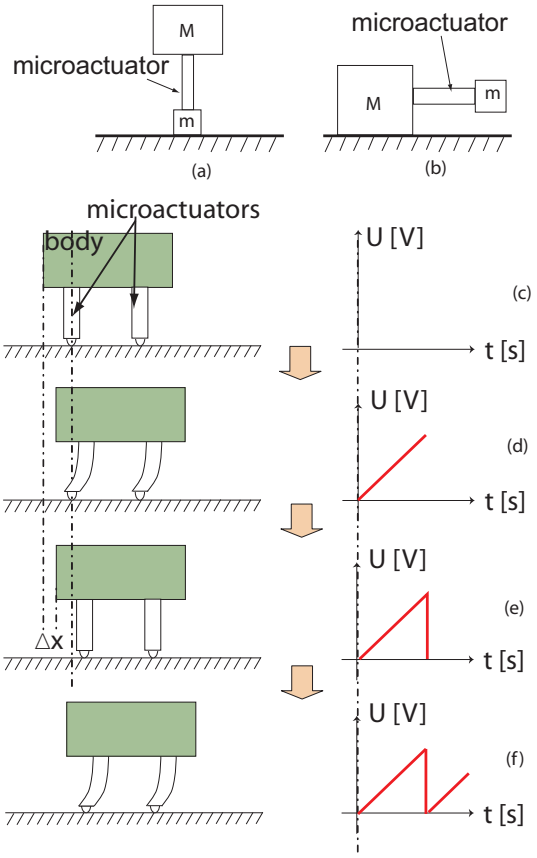

Fig. 3. The inertial-drive principles: (a) stick-slip, (b) impact-drive.

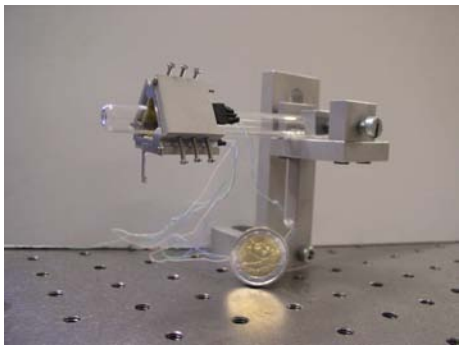

Fig. 4. A stick-slip micropositioning system based that can perform linear and angular motions on its support [13].

IV. The nonlinear behavior of the microactuators

Active materials, such as piezoelectric and Shape Memory Alloy materials, exhibit nonlinearities when used in certain conditions. These nonlinearities, which are usually the hysteresis and the creep, indeniably influence the repeatability and the accuracy of the microactuators. While the effects of these nonlinearities can be efficiently rejected by using feedback controllers [18][19], the lack of convenient sensors leads researchers to use feedforward (or open-loop) controllers [20][21][22]. For

nanopositioning, a survey of recent control techniques is illustrated in [23]. Fig. 5 pictures the hysteresis and the creep of a piezoelectric cantilever dedicated to microassembly/and micromanipulation tasks. As shown in the figure, the hysteresis is a characteristic in the input-output transfer while the creep is defined as the drift that appears when a constant input is applyed.

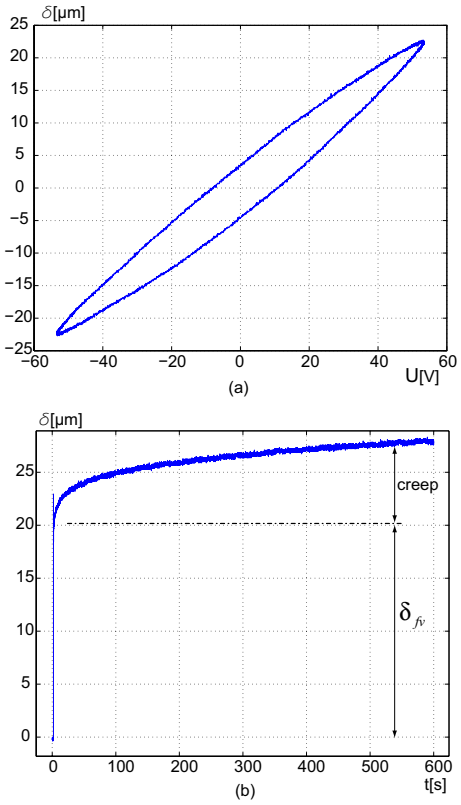

Fig. 5. Nonlinear behavior of a piezoelectric cantilever dedicated to micromanipulation/microassembly tasks [22].

V. The need of visual feedback systems

Because of the smallness of the objects, it is impossible for a human operator to directly visualize the scene. This is why camera-microscope-screen systems are usually used in micromanipulation/microassembly tasks. They permits a visual feedback furing a teleoperated task [25]. In some cases, a virtual reality technique is coupled with camera-microscope-screen system in order to well reconstruct the environment and the phenomena of the microworld [26].

Camera-microscope systems are also of great interest in automated micromanipulation/microasembly systems. Indeed, these tasks are very sensitive to the environment, especially to the dusts (whoses sizes are comparable to the manipulated micro-objects), the air-flow, the humidity and the temperature [27]. One solution is to use a controlled environment station [28] but if a camera-microscope system is present for visual feedback, it can be used to complete the automation of the station. Many algorithms and studies have been brought in this aim for microworld applications [29][30]. Fig. 6 pictures a micromanipulation station equiped with a camera-microscope system [31].

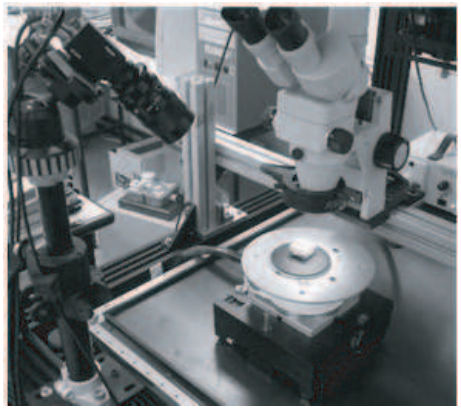

Fig. 6. A micromanipulation station equiped with a camera-microscope system [31].

VI. The high sensitivity to noises and disturbances

Systems working in the microworld are known to be very sensitive to noises and disturbances. Indeed, the order of magnitude of the specified displacements (less than $100\mu m$) are similar to that of the displacement due to noises/disturbances. They are often due to environmental disturbances (thermal variation, vibration, airflow, humidity variation). As example, Fig. 7 illustrates the significance of the noise in a recorded signal corresponding to the position of a micromanipulator and using a strain gauge measurement [32]. In the reference, the accuracy of the measured signal (nearly $3\mu m$) is considered to be bad whereas the specified accuracy should be sub-micrometric. Hence, filtering techniques have been used to improve the quality of the signal.

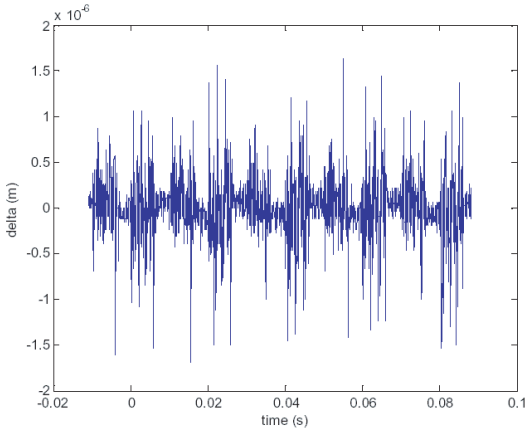

Fig. 7. The significance of the noise in micromanipulators signals [32].

TABLE I

Sensor types currently used in many microworld applications.

	overshoot	settling time
Sensor type	Advantages	Drawbacks
Triangulation lasers	High precision and resolution, good band pass	Quite expensive, large sizes, limited measurement ranges.
Interferometers	Very high resolution, high accuracy and high range	Very expensive, large sizes
Strain gages	Reduced sizes, cheap	Fragile, noisy output signal
Integrated capacitive	High sensitivity, high precision, convenient sizes	Nonlinear
Piezoelectric	High band pass, high precision	Nonlinear, no static measurements
Piezomagnetic		Nonlinear, dimensions
Image processing	Large measurement range	Expensive, bulky

VII. Conclusion

Many tasks in the microworld require very high performances such as nanometric resolution, micro/nanometric accuracy, millisecond response time, etc. To reach these specifications, the use of convenient sensors is indispensable. But until now, sensors that have suitable sizes, high accuracy and high dynamics do not exist neither un industry nor in research. Table I resumes the sensors used for the measurement of force and displacement in many microworld applications.

The development of accurate, high band pass and easily integrable sensors needs to be developped. In parallel, the research advances in control techniques design for micro/nano-world has to be continued.

References

[1] J. Bryzek, E. Abbott, A. Flannery, D. Cagle and J. Maitan, 'Control issues for MEMS', IEEE Conference on Decision and Control (CDC), pp.3039-3047, Hawaï USA, Decembe 2003.

[2] Y. Sun and B. J. Nelson, 'Microrobotic cell injection', IEEE International Conference on Robotics and Automation (ICRA), pp.620-625, Seoul Korea, May 2001.

[3] S. Park, K. Costa and G. Ateshian, 'Microscale frictional response of bovine articular cartilage from atomic force microscopy', Elsevier Journal of Biomechanics, vol. 37, No11, pp.1679-1687, November 2004.

[4] M. Girot, M. Boukallel and S. Régnier, 'A micro and nanoforce biomicroscope device for in vitro mechanotransduction investigation', IEEE Transaction on Instrumentation and Measurement, pp.2532-2541, 2008.

[5] Y. Bellouard, R. Clavel, R. Gotthardt, J. E. Bidaux and T. Sidler, 'A new concept of monolithic shape memory alloy microdevices used in microrobotics', International Conference on New Actuators, Bremen Germany, June 1998.

[6] J. Abadie, N. Chaillet and C. Lexcellent, 'Bending model of an integrated SMA micro-actuator', Journal of Intelligent Material System and Structures, Vol.15, No8, pp.601-609, 2004.

[7] J. Y. Gauthier, A. Hubert, N. Chaillet and C. Lexcellent, 'Modeling and control of micro-mechatronicdevices: application of variational and energetic methods for micro-actuator design', 7th France-Japan and 5th Europe-Asia Congress Mecatronics, 2008.

[8] R. Letenberg, A. W. Groeneveld and M. Elwenspoek, 'Comb-drive actuator for large displacements', Journal of Micromechanics and Microengineering, Vol.6, pp.320-329, 1996.

[9] Y. Haddab, N. Chaillet and A. Bourjault, 'A microgripper using smart piezoelectric actuators', IEEE/RSJ International Conference on Intelligent Robots and Systems (IROS), pp.659-664, Takamatsu Japan, November 2000.

[10] Z. Hua, H. Honglin, L. Huafeng and Z. Chunsheng, 'Development of a novel piezoelectric micromotor', Journal of Electrical Engineering, vol.58, No3, pp.169-172, 2007.

[11] D. O. Popa, B. H. Kang, J. T. Wen, H. E. Stephanou, G. Skidmore and A. Geisberger, 'Dynamic Modeling and Open-Loop Control Of Thermal Bimorph MEMS Actuators', IEEE International Conference on Robotics and Automation (ICRA), Taipei, Taiwan, 2003.

[12] W. Driesen, A. Bergander, T. Varidel and J. M. Breguet, 'Energy consumption of piezoelectric actuators for inertial drives', IEEE International Symposium on Micromechatronics and Human Science, pp.51-58, 2003.

[13] M. Rakotondrabe, Y. Haddab and P. Lutz, 'Development, modeling and control of a micro/nanopositioning 2-dof stick-slip device', IEEE Transaction on Mechatronics, to appear 2009, (VOL.14), doi: 10.1109/TMECH.2008.2011134.

[14] S. Fatikow, T. Wich, H. Hülsen and M. M. Jähnisch, 'Microrobot system for automatic nanohandling inside a scanning electron microscope', IEEE Transaction on Mechatronics, Vol.12, No3, pp.244-252, 2007.

[15] J. M. Breguet and R. Clavel, 'Stick and slip actuators: design, control, performances and applications', IEEE International Symposium on Micromechatronics and Human Science, pp.89-95, 1998.

[16] B. Sedghi, 'Control design systems via dehybridization', PhD dissertation, Ecole Polytechnique Fédérale de Lausanne, Lausanne Switzerland, 2003.

[17] M. Rakotondrabe, Y. Haddab and P. Lutz, 'Voltage/frequency proportional control of stick-slip microsystems', IEEE Transactions on Control Systems Technology, Vol.16, Issue 6, pp:1316-1322, 2009.

[18] H. Numasato and M. Tomizuka, 'Settling control and performance of dual-actuator system for hard disk drives', Amercian Control Conference, pp.2779-2785, 2001.

[19] M. Rakotondrabe, Y. Haddab and P. Lutz, 'Quadrilateral modelling and robust control of a nonlinear piezoelectruc cantilever', IEEE Transaction on Control Systems Technology, Vol.17, to appear 2009.

[20] D. Croft, G. Shed and S. Devasia, 'Creep, hysteresis and vibration compensation for piezoactuators: atomic force microscopy application', ASME Journal of Dynamic Systems, Measurement and Control, 2001.

[21] B. Mokaberi and A. A. G. Requicha, 'Compensation of scanner creep and hysteresis for AFM nanomanipulation', IEEE Transaction on Automation Science and Engineering, pp.197-208, 2008.

[22] M. Rakotondrabe, C. Clévy and P. Lutz, 'Complete open loop control of hysteretic, creeped and oscillating piezoelectric cantilevers', IEEE Transaction on Automation Science and Engineering, to appear 2009.

[23] S. Devasia, E. Eleftheriou and S. O. R. Moheimani, 'A survey of control issues in nanopositioning', IEEE Transaction on Control Systems Technology, Vol.15, No5, pp.802-823, 2007.

[24] M. Gauthier, S. Régnier, P. Rougeot and N. Chaillet, 'Forces

analysis for micromanipulations in dry and liquid media', Journal of MicroMechatronics, Vol.3, pp.389-413, 2006.
[25] Q. Zhou, P. Kallio and K. N. Koivo, 'Virtual environment for operations in the microworld', SPIE, 2000.
[26] M. Ammi and A. Ferreira, 'Virtualized reality interface for telemicromanipulation', IEEE International Conference on Robotics and Automation (ICRA), pp.2776-2781, New-Orleans USA, 2004.
[27] Q. Zhou, C. del Corral, P. J. Esteban and K. N. Koivo, 'Environmental influences on microassembly', IEEE/RSJ International Conference on Intelligent Robots and Systems (IROS), 2002.
[28] Q. Zhou, A. Aurelian, C. del Corral, P. J. Esteban, P. Kallio, B. Chang and K. N. Koivo, 'A microassembly station with controlled environment', SPIE Photonics, 2001.
[29] G. Yang, J. Gaines and B. J. Nelson, 'A supervisory wafer-level 3D microassembly system for hybrid MEMS fabrication', Journal of Intelligent and Robotic Systems, Vol.37, pp.43-68, 2003.
[30] B. Tamadazte, S. Dembélé, G. Fortier and N. Le Fort-Piat, 'Automatic micromanipulation using multiscale visual servoing', IEEE International Conference on Automation Science and Engineering (CASE), Washington USA, 2008.
[31] A. Shackslock and W. Sun, 'Integrating microscope and perspective views', IEEE International Conference on Robotics and Automation (ICRA), Barcelona Spain, April 2005.
[32] Y. Haddab, Q. Chen and P. Lutz, 'Improvement of strain gauges micro-forces measurement using Kalman optimal filtering', International Journal of IFAC Mechatronics, to appear 2009, doi:10.1016/j.mechatronics.2008.11.012.

Force control for nanohandling inside Scanning Electron Microscopes

Daniel Jasper

***Abstract*— This work describes a new approach for measuring the applied force during nanohandling operations making use of a newly available position tracking technique. With special target patterns structured on the tools, the applied force can be measured using the scanning electron microscope without requiring additional cabling. The concept is proven by appying force to a carbon nanotube with a customized electrothermal gripper. Furthermore, the exceptional update rate and resolution of the sensor suggest that simple control algorithms are sufficient to apply precise forces in the nN-range.**

I. Introduction

In addition to reliable microrobot positioning [1], [2], applying a controllable amount of force during a nanohandling or -assembly operation is essential for the reliability of the operation itself as well as the resulting product. E.g., excessive force generated by a nanogripper could damage the handled object and thus make the resulting product unusable. Insufficient force on the other hand can lead to improper gripping and thus misalignment or loss of the object. Integrating force sensors into micro- or nanotools, however, is difficult. Due to the required small size, possible force sensing mechanisms such as piezoresistive feedback are noisy, have a limited dynamic range, could be influenced if hit by the electron beam of a scanning electron microscope (SEM) and require tedious wiring.

Due to the required visual feedback, most nanoscale operations are currently performed in an SEM. With the approach presented in [3], it is possible to obtain highly dynamic position information using the SEM as position sensor. Simultaneously tracking a fixed point and the end of a well-known bending structure such as a cantilever or a gripper jaw, the applied force can also be measured with a high update rate and high resolution. Thus, it is possible to integrate precise force sensors into virtually every nanotool used for SEM-based nanohandling without complicating the tool's manufacturing process or requiring additional cabling.

This works describes the implementation of the SEM-based position tracking approach and the first prototype of a force-sensing gripper. First results obtained with this gripper are presented. Preliminary tests with an electrothermal microgripper handling a multi-walled carbon nanotube have shown that a simple PID controller is sufficient to control the exerted force. The patterns required for position tracking could easily be created on the gripper using electron beam-induced deposition [5]. A comparison to a cantilever with piezoresistive readout has shown the approach's advantages in terms of noise and accuracy.

II. Implementation

In order to effectively utilize the approach described in [3], a custom scan generator was required. A scan generator actuates the scanning coils of the SEM with two analog voltages and captures the detectors signal. The newly built scan generator allows for a real-time scan of arbitrary lines and thus offers the flexibility to move the electron beam with the exact pattern required for tracking multiple target patterns with a very high update rate.

The scan generator was built using a field programmable gate array (FPGA) for the digital signal generation. Thus, it can quickly be adapted to changing requirements of the tracking algorithm. The digital signals are then converted using high-speed digital-to-analog converters (DACs). The output of the SEM's detector is digitized using a high-speed analog-to-digital converter (ADC) and fed back into the FPGA for further evaluation. Currently, all of the acquired data is then sent to a PC, but it will also be possible to perform the calculation of the tracking algorithm using dedicated hardware on the FPGA in order to improve the performance and response time.

In comparison to the tracking algorithm described in [3], a simplified scanning pattern was used (see Fig. 1). Basically, just one horizontal and one vertical line scan are used to determine a pattern's position. There are two downsides to this approach. Firstly, only the x- and y-position of the pattern can be calculated, the rotational degree of freedom is not measured. Secondly, because the pattern is not continuous, the electron beam needs to perform rapid movements leading to a short delay for beam settling. The downsides are not critical for force measurements. The tracked pattern, however, can be simplified to a single circular area, which can easily be created using point-shaped electron beam-induced depositions (EBiD). Several of these point-shaped

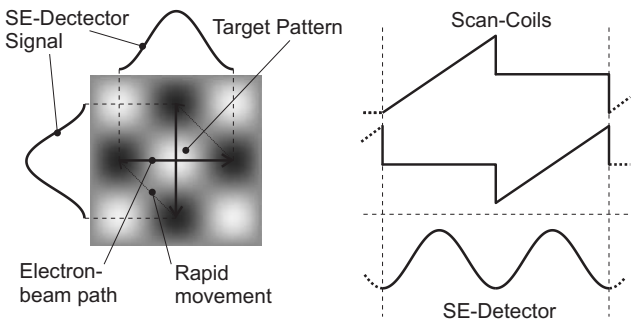

Fig. 1. Simplified scanning pattern to position of a circular target.

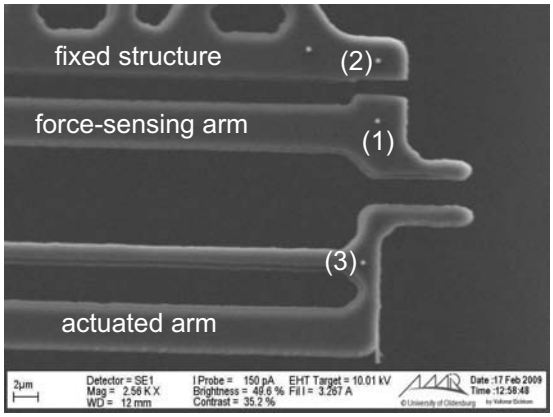

Fig. 2. Force-sensing gripper with applied EBiD patterns.

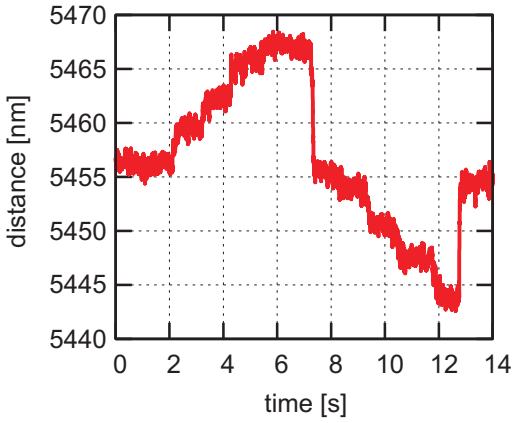

Fig. 4. Force measurements when pushing a CNT against a gripper jaw.

depositions are created on the tips of an electrothermal microgripper [4] as shown in Fig. 2. For force measurements, the patterns (1) and (2) are used. With the additional pattern (3), the current gripper opening can be monitored.

Pattern (1) was applied to a gripper jaw that is attached to the silicon substrate with a rectangular silicon beam of 150x5x4 μm^3. The spring constant k for this cantilever can be calculated with:

$$k = \frac{E \cdot w \cdot h^3}{4 \cdot l^3} \approx 4\,\text{N/m},$$

with Young's modulus E (approx. 169 GPa for silicon), width w, height h and length l. Pattern (2) is applied to a rigid structure also connected to the silicon substrate and can thus be used as a fixed reference. The bending of the cantilever can now simply be monitored be measuring the distance of the two patterns.

III. Results

As a first characterization measurement, the tip of a multi-walled carbon nanotube (CNT) was pushed against the force-sensing gripper jaw (see Fig. 3). The measured distance of the two reference points can be seen in Fig. 4. In 1 μm steps, the CNT was increasingly bent against the gripper until it flipped to the other side (one step after Fig. 3b). Then the same movement was preformed into the opposite direction. As can be seen, the measured force increased linearly with a maximum displacement of the gripper jaw by 12 nm. Using the spring constant derived above, this corresponds to approximately 60 nN. The noise on the measured value is roughly 2 nm corresponding to 8 nN for the given silicon beam. However, several tradeoffs have to be considered. Firstly, there is a tradeoff between speed and resolution. In order to get the noise level down to 2 nm, a 10-fold average filter was used. Thus, the update rate of a sensor with that resolution is limited to 100 Hz. Using the full update rate of 1 kHz leads to approximately 10 nm resolution (40 nN). Secondly, the stiffness of the silicon beam has to be chosen carefully. If it is too soft, the gripper cannot generate sufficient force, while the resolution is limited, if it is too hard.

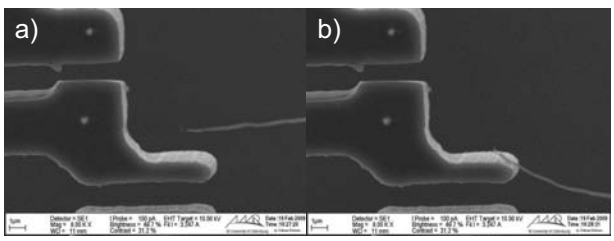

Fig. 3. Pushing a CNT against a gripper jaw: a) unloaded and b) maximum force before flipping to the other side.

IV. Conclusion

This work proves the concept of a new approach to force control. Firstly, a custom scan generator can be used to track small patterns generated using EBiD. The tracking exhibits a high update rate (up to 1 kHz) with high resolution (down to 2 nm). Differentially measuring two of such patterns on a known structure, force measurements can be conducted. Thereby, nanotools can be enhanced with force sensors without the need of cabling. The resolution obtained with the first prototype was 8 nN but can be enhanced using softer bending structures.

References

[1] T. Sievers and S. Fatikow, "Visual servoing of a mobile microrobot inside a scanning electron microscope," in *IEEE/RSJ International Conference on Intelligent Robots and Systems (IROS)*, Aug. 2005, pp. 1350–1354.

[2] T. Sievers, M. Jähnisch, C. Schrader, and S. Fatikow, "Vision feedback in an automatic nanohandling station inside an SEM," in *6th Int. Optomechatronics Conference on Visual/Optical Based Assembly and Packaging, SPIE's Optics East*, Oct. 2006.

[3] D. Jasper, "High-speed position tracking for nanohandling inside Scanning Electron Microscopes," in *Proceedings of ICRA 2009, accepted*, 2009.

[4] O. Sardan, V. Eichhorn, D. Petersen, S. Fatikow, O. Sigmund, and P. Bøggild, "Rapid prototyping of nanotube-based devices using topology-optimized microgrippers," *Nanotechnology*, vol. 19, p. 9, 2008.

[5] T. Wich, T. Sievers, and S. Fatikow, "Assembly inside a scanning electron microscope using electron beam induced deposition," in *Proc. Int. Conf. on Intelligent Robots and Systems (IROS'06)*, Beijing, China, October 2006, pp. 294–299.

Controlled Optical Trapping for Nanoparticles

Jason J. Gorman, *Member, IEEE*, Thomas W. LeBrun, and Arvind Balijepalli,

Abstract— Optical trapping is a technique in which optical forces are used to manipulate particles ranging in diameter from 20 µm to 20 nm. It has been used extensively in biophysics research, including the characterization of the mechanical properties of DNA, as well as in the measurement of physical properties of nanoparticles. Controlling the position of a trapped particle when performing measurements such as these is critical to their success, where positioning resolution on the order of nanometers is typically required. However, Brownian motion caused by the thermal interaction between the surrounding medium and the trapped particle limits the open-loop positioning resolution, thereby necessitating the use of feedback control. This presentation will examine the closed-loop control of optically trapped nanoparticles for the suppression of Brownian motion. An overview of several control schemes will be presented including a method which minimizes Brownian motion while limiting the maximum control activity. Experimental control results demonstrate a 73 % reduction in the maximum amplitude for the Brownian motion of an optically trapped silica sphere with a diameter of 0.97 µm over a range between 10 Hz and 6.4 kHz.

I. Introduction

OPTICAL trapping is a technique in which focused light, typically from a laser, is used to impart forces on microscopic objects, providing an efficient method for localizing and manipulating particles with dimensions from 20 µm to 20 nm. The single-beam gradient force optical trap, which is the most common approach for optical trapping and is also the approach discussed in this presentation, was first reported by Ashkin et al. [1]. Since then, a number of variations on this approach have been developed for specific applications in biophysics, colloidal science, and nanotechnology (see Visscher, Gross, and Block [2], Ashkin [3], and Grier [4] for an overview). In particular, optical trapping has been critical in the measurement of force and displacement characteristics of motor proteins in various biological processes [5-8].

One limitation in utilizing optical trapping in many applications is the Brownian motion exhibited by a particle within an optical trap. An optical trap can be approximately modeled as a potential well with finite depth. A particle inside the trap experiences thermal noise due to constant bombardment by the molecules that comprise the fluid, resulting in random motion of the trapped particle. Furthermore, if the thermal energy of the particle is large enough, the particle will reach the top of the potential well and escape from the trap. The Brownian motion of the particle inside the trap limits the precision at which biophysical measurements can be made and nanoscale structures can be assembled.

Interestingly, control systems have been a part of optical trapping research since the early stages of development, as seen in the optical levitation experiments by Ashkin and Dziedzic [9]. Other researchers have followed suit in their integration of control systems and optical trapping, resulting in several variations on controlled optical trapping [5-8], [10]-[17]. However, with the exception of Simmons et al. [10], the presented controllers do not have the necessary bandwidth to suppress Brownian motion at a useful level over the entire bandwidth of the particle motion. Furthermore, the control theoretic aspects of this problem have only been considered by Ranaweera and Bamieh [13], [15] and Wulff, Cole, and Clark [14], [16], [17].

In this extended abstract, a closed-loop control approach for optical trapping which can dramatically reduce this limitation by suppressing the Brownian motion within the frequency band of interest in many trapping experiments is discussed (for further details see [18, 19].) Additional modeling and control approaches will also be presented as part of the "Control Issues in the Micro/Nano-World" workshop.

II. System Description

A schematic of an optically trapped particle is shown in Fig. 1. When the optical forces (scattering and gradient forces) are balanced, the particle has an equilibrium position located near the focal spot of the trapping laser. The particle can be manipulated in the *XY* plane by scanning the trapping laser, thereby changing the position of the focal spot. The trapping force can be modeled as a nonlinear spring that connects the particle to the trap position. Therefore, when the trap moves, the particle will also move. The control approach described here uses this interaction to impart forces on the trapped particle in order suppress the particle's Brownian motion.

A block diagram representation of the dynamics along the x axis for an optically trapped particle is shown in Fig. 2 (the y axis dynamics are similar). The position of the trap, x_t, directly influences the position of the particle, x. In this case, x_t, is controlled using an acousto-optic deflector (AOD), which can scan the trap laser with a bandwidth up to 30 kHz. A controllable function generator provides a radio frequency (RF) signal proportional to the desired scan angle of the AOD, which is then amplified and supplied to the AOD. The dynamics of this scanning hardware can be neglected in the bandwidth of interest, and can be modeled by a simple proportional gain.

J. J. Gorman*, T. W. LeBrun, and A. Balijepalli are with the Manufacturing Engineering Laboratory, National Institute of Standards and Technology, Gaithersburg, MD 20899 USA (*corresponding author, e-mail: gorman@nist.gov).

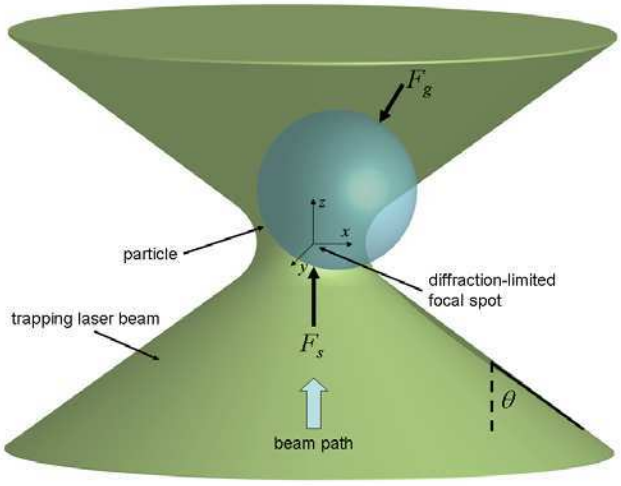

Fig. 1 Diagram of an optically trapped particle. The gradient forces, F_g, push the particle to the center of the trap while the scattering forces, F_s, push the particle along the optical axis. When the gradient forces are greater than the scattering forces the trap is stable.

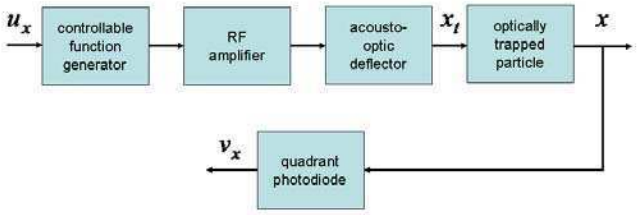

Fig. 2 Block diagram of the trapping instrumentation

The position of the particle is measured in the *XY* plane using back focal plane detection (see [2]). This is a laser-based method that images the particle onto a quadrant photodiode, and can measure the position of the particle with nanometer resolution. The output of this sensing system is a voltage proportional to position. Returning to Fig. 2, it can be seen that the frequency command input to the function generator, u_x, is the control input, and the detection system signal, v_x, is the system output. The goal of the control design discussed in the next section is to suppress the particle Brownian motion by closing the loop between these two variables.

III. Control Design

The closed-loop control diagram for this system is shown in Fig. 3, where r_x is the desired particle position (usually zero), Γ_x is the thermal noise input, $G_d(s)$ and $G_p(s)$ represent the dynamics of the trapped particle, and $G_c(s)$ is the controller. In this case, an analog proportional-integral-derivative (PID) controller is used with gains K_p, K_i, and K_d, respectively. Using a linearized first-order model of the trapped particle, and the PID controller, the transfer function between Γ_x and x can be written as

$$G_{\Gamma_x x}(s) = \frac{bs}{\left(1+\bar{a}\,K_d\right)\,s^2 + \left(a+\bar{a}\,K_p\right)\,s + \bar{a}\,K_i} \tag{1}$$

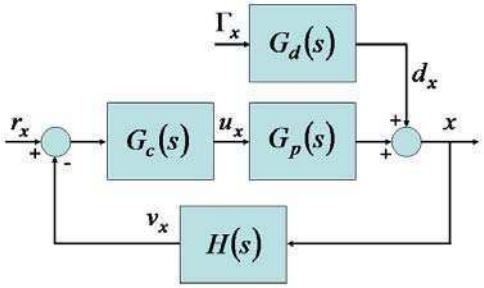

Fig. 3 Block diagram of closed-loop system

where a, $\bar{a}$, and b are system parameters. The main goal of the controller design is to maximize the suppression of Brownian motion, both in terms of the maximum amplitude and the root mean squared (rms) motion. The H_∞ and H_2 norms of Eqn. (1) provide these two parameters, respectively. They have been calculated analytically, such that

$$\left\|G_{\Gamma_x x}\right\|_\infty = \frac{b}{a+\bar{a}\,K_p} \tag{2}$$

$$\left\|G_{\Gamma_x x}\right\|_2 = \frac{b}{\sqrt{2\left(a+\bar{a}\,K_p\right)\left(1+\bar{a}\,K_d\right)}} \tag{3}$$

From Eqn. (2), it is clear that the maximum amplitude of the Brownian motion can only be reduced by increasing K_p. However, from Eqn. (3), it is shown that the rms Brownian motion can be reduced by increasing either K_p or K_d. As would be expected, the integral control action does not reduce the motion caused by thermal noise. These results provide a clear method for tuning the control gains to suppress Brownian motion. However, nonlinearities not considered in the analysis can cause instabilities when the gains are set too high.

IV. Experimental Results

The controller discussed in the previous section was implemented on a custom optical trapping instrument and was used to trap 0.97 μm diameter silica particles. The optical power of the trapping laser during these experiments was 130 mW. A number of different gain combinations were tested and the power spectra for the output of the position detection system were recorded. From these power spectra, the maximum amplitude (~ H_∞) and rms motion (~ H_2) of the trapped particle were calculated. These results are shown in Table I, and the power spectra for P and PD control are shown in Figs. 4 and 5.

These results confirm the analysis from Eqns. (2) and (3). The maximum amplitude of Brownian motion does decrease with increasing K_p, as seen in Fig. 4. Additionally, K_d can be used to reduce the rms motion compared to a proportional controller (see Fig. 5). The PD controller results in a 73 % reduction in the maximum amplitude for the Brownian

Table I

H_∞ and H_2 norms of particle Brownian motion for various PID gains

Case	Gains	$\left\|G_{\Gamma_x x}\right\|_\infty$	$\left\|G_{\Gamma_x x}\right\|_2$
1	Open Loop	0.0282	0.0395
2	$K_p = 7.6$	0.0109	0.0286
3	$K_p = 10.0$	0.0115	0.0267
4	$K_p = 13.6$	0.0090	0.0248
5	$K_p = 19.6$	0.0077	0.0220
6	$K_p = 10.0$, $K_d = 3.5e^{-4}$	0.0119	0.0232
7	$K_p = 19.6$, $K_i = 2000$	0.0077	0.0242

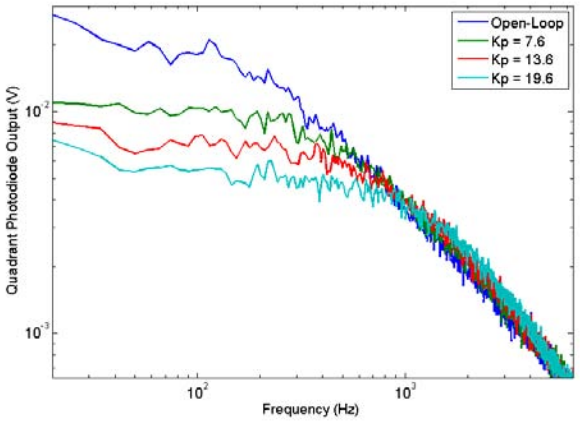

Fig. 4 Proportional control: Brownian motion amplitude for several values of K_p

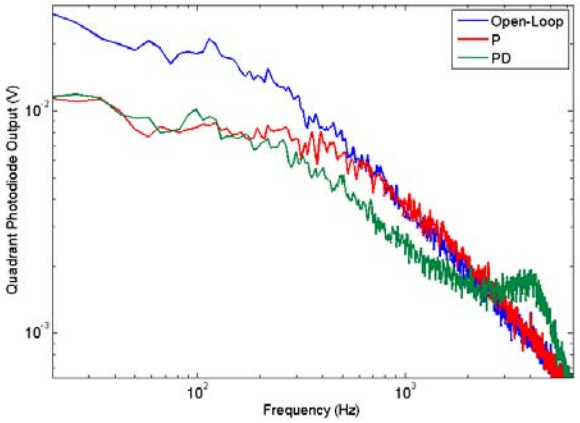

Fig. 5 Comparison between proportional (P) and proportional-derivative (PD) controllers

motion over a frequency range between 10 Hz and 6.4 kHz. These results demonstrate the effectiveness of closed-loop optical trapping when the controller is designed to have sufficient bandwidth to counteract the thermal noise. In the presentation, other control approaches that utilize additional control inputs, including the laser power, will also be discussed. Additionally, the effects of using different beam steering and modulation hardware on the closed-loop dynamics will be addressed.

REFERENCES

[1] Ashkin, J. M Dziedzic, J. E. Bjorkhom, and S. Chu, "Observation of a single-beam gradient force optical trap for dielectric particles," *Optics Letters*, vol. 11, pp. 288-290, 1986.

[2] K. Visscher, S. P. Gross, and S. M. Block, "Construction of multiple-beam optical traps with nanometer-resolution position sensing," *IEEE Journal of Selected Topics in Quantum Electronics*, vol. 2, pp. 1066-1076, 1996.

[3] A. Ashkin, "History of optical trapping and manipulation of small-neutral particle, atoms, and molecules," *IEEE Journal on Selected Topics in Quantum Electronics*, vol. 6, pp. 841-856, 2000.

[4] D. G. Grier, "A revolution in optical manipulation," *Nature*, vol. 424, pp. 810-816, 2003.

[5] J. T. Finer, R. M. Simmons, and J. A. Spudich, "Single myosin molecule mechanics: piconewton forces and nanometer steps," *Nature*, vol. 368, pp. 113-119, 1994.

[6] M. D. Wang, H. Yin, R. Landick, J. Gelles, and S. M. Block, "Stretching DNA with optical tweezers, Biophysical Journal, vol. 72, pp. 1335-1346, 1997.

[7] M. D. Wang, M. J. Schnitzer, H. Yin, R. Landick, J. Gelles, and S. M. Block, "Force and velocity measured for single molecules of RNA polymerase," *Science*, vol. 282, pp. 902-907, 1998.

[8] S. M. Block, C. L. Asbury, J. W. Schaevitz, and M. J. Lang, "Probing the kinesin reaction cycle with a 2D optical force clamp," *Proceedings of the National Academy of Sciences*, vol. 100, pp. 2351-2356, 2003.

[9] A. Ashkin and J. M. Dziedzic, "Feedback stabilization of optically levitated particles," *Applied Physics Letters*, vol. 30, pp. 202-204, 1977.

[10] R. M. Simmons, J. T. Finer, S. Chu, and J. A. Spudich, "Quantitative measurements of force and displacement using an optical trap," *Biophysical Journal*, vol. 70, pp. 1813-1822, 1996.

[11] K. Visscher and S. M. Block, "Versatile optical traps with feedback control," *Methods in Enzymology*, vol. 298, pp. 460-489, 1998.

[12] M. J. Lang, C. L. Asbury, J. W. Shaevitz, and S. M. Block, "An automated two-dimensional optical force clamp for single molecule studies," *Biophysical Journal*, vol. 83, pp. 491-501, 2002.

[13] A. Ranaweera, B Bamieh, and A. R. Teel, "Nonlinear stabilization of a spherical particle trapped in an optical tweezer," *IEEE Conference on Decision and Control*, Maui, HI, 2003, pp. 3431-3436.

[14] K. D. Wulff, D. G. Cole, and R. L. Clark, "Development of precision optical traps for single molecule and motor protein research," *ASME International Mechanical Engineering Congress and Exposition*, Anaheim, CA, 2004, IMECE2004-61800.

[15] A. Ranaweera and B. Bamieh, "Modeling, identification, and control of a spherical particle trapped in an optical tweezer," *International Journal of Robust and Nonlinear Control*, vol. 15, pp. 747-768, 2005.

[16] K. D. Wulff, D. G. Cole, and R. L. Clark, "Servo control of an optical trap," *Applied Optics*, vol. 46, pp. 4923-4931, 2007.

[17] K. D. Wulff, D. G. Cole, and R. L. Clark, "Adaptive disturbance rejection in an optical trap," *Applied Optics*, vol. 47, pp. 3585-3589, 2008.

[18] J. J. Gorman, T. W. LeBrun, and A. Balijepalli, "Control of optically trapped particles for Brownian motion suppression," *IEEE Transactions on Control Systems Technology*, accepted for publication, 2009.

[19] J. J. Gorman, T. W. LeBrun, and A. Balijepalli, "Controlled Optical Trapping: Instrumentation, Methods, and Applications," in *Feedback Control at the Micro- and Nano-Scales: MEMS to Atoms*, J. J. Gorman and B. Shapiro, Eds., New York: Springer, 2010.

Precision-Driven Hybrid Control for 3D Microassembly

Dan O. Popa, Aditya N. Das

Abstract— In recent years, several research groups around the world have demonstrated 3D assembly and manipulation tasks in the micro and nano domain, performed semi-autonomously or autonomously with the help of precision robots. Notable applications include the assembly of MEMS and NEMS sensors and actuators, micro and nano robots, and biological samples. In virtually all cases, research has focused on the feasibility of using top-down automation to perform the required tasks with the required precision. However, the type of control strategy employed in such cases is both part-specific, as well as assembly station specific, and does not take into account important quality factors that are routinely employed macro domain automation. In recent work, we introduced quantitative metrics (the High-Yield Assembly Condition, HYAC), leading to rules for selection of precision robots in microassembly cells (Resolution-Repeatability-Accuracy Rules, RRA). In this presentation, we make use of such metrics and rules to formulate a precision-adjusted hybrid controller. The controller is used as a decision framework to select efficient control strategies during microassembly. We will present several benchmark simulations and experimental examples indicating that the use of such a controller can lead to high yields, faster speeds, and to the use of fewer sensors during top-down automated microassembly.

I. MICROSCALE ASSEMBLY

UNLIKE semiconductor integrated circuits (ICs), newer microsystems combine sensors, actuators, mechanical structures, electronics, and optics on a single substrate. In such a diversified system, heterogeneous manipulation of components become unavoidable as structural complexity of MEMS grows. In an effort to find a solution to reduced yields and speeds in manufacturing at the micro-scale, research initiated in 1990s has sought to understand top-down aspects of micromanipulation, sensor-based precision control of robots, self alignment effects using compliant micro structure designs, and so on.

Several papers describe and classify the architecture and algorithms used in high precision robotic cells for the purpose of directed microscale assembly [1-6]. Multi-scale assembly methods can be classified based on throughput (serial or parallel), deliberate intervention (deterministic or stochastic), type of end-effectors (contact, non-contact) or level of human intervention (manual, teleoperated or automated). Many examples of the use of microgrippers to manipulate compliant microparts can be found, including passive grippers [3], thermally, electrostatic, or piezoelectric actuated microgrippers [7], the use of adhesive forces for micromanipulation [8], or active surface manipulators [9].

Out-of-plane manipulation of micro-sized parts using high precision robots offers flexibility to integrate different materials, have comparatively simpler design and smaller real-estate, and use reconfigurable modular structures. However automated microassembly also requires adressing control and planning related challenges [13]. Higher volume production of miniaturized devices requires the successful operation at required throughput and yield across multiple scales of tolerance, part dimension and workspace limitations.

In this presentation we focus on the supervisory control of automated deterministic serial microassembly. Typically, sequential microassembly requires a high precision micromanipulator and motion control; either by off-line programming with calibration or by on-line sensory feedback control. The later can be accomplished via a microscope or a force sensor integrated with the gripper, or both. However, the price paid in assembly speed is considerable, resulting in low assembly throughputs. On the other hand, open loop control does not necessarily ensure high assembly yields, especially in case of complex and sequential processes.

A hybrid controller is proposed to take advantages of both precision control methods. The use of hybrid control is a widely adopted in macro scale for a variety of control applications [10, 11], but relatively few applications use it at small scales, with the notable exceptions of vibration suppression [12]. We present experimental results indicating that the hybrid controller achieves 35% more accuracy than pure open loop control, while the assembly throughput is 60% faster that pure closed-loop control.

II. MICROSCALE ASSEMBLY

A. Microspecrometer Assembly with μ³

Manufacturing of a complex and heterogeneous microsystem involves several steps such as design, fabrication, assembly, packaging, testing etc. Generally these processes are established in a highly unrelated manner, but this can lead to low yields later on. Whereas at the macro scales, automation is often undertaken after, and often benchmarked against manual assembly, deterministic automation at the MEMS scale requires a more holistic approach. This means that the designs of the assembly cell, part and end-effectors should be considered simultaneously,

Manuscript received March 1, 2009. The authors are with Automation and Robotics Research Institute, The University of Texas at Arlington, TX, USA. (e-mail: popa@uta.edu)

and that by doing so, we can automate assembly operations in a realistic manner by ensuring higher process yield, lower cycle time and lesser sensor overhead.

As a case study for the proposed controller we consider the automated assembly of a *microspectrometer,* a complex MOEMS (micro-opto-electo-mechanical-systems) sensor for wide range spectrum analysis and gas detection applications [14].

A microrobotic system - *"μ^3"* has been configured at ARRI's Texas Microfactory Labs to carry out general microassembly tasks (Figure 1). It consists of three robotic manipulators with 19 DOF, four high magnification microscopes to provide stereo vision for tele-operated as well as visual servoing [15].

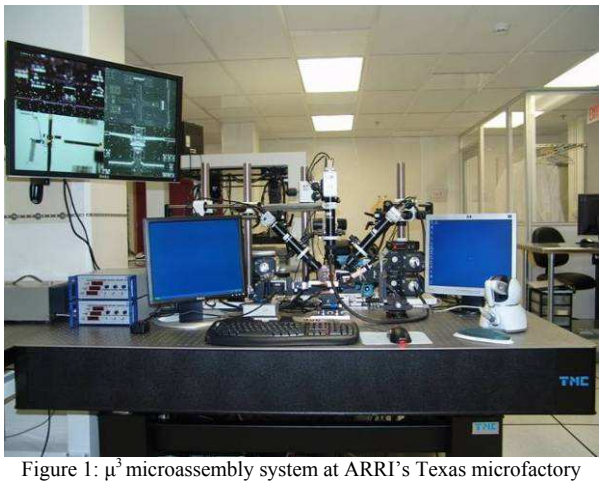

Figure 1: μ^3 microassembly system at ARRI's Texas microfactory

Automated microassembly of the microspectrometer using the μ^3 poses unique challenges, because multiple heterogeneous micro-components need to be assembled with a tight mechanical as well as optical alignment. Compliant part and socket designs are used to snap-fit several 2½D silicon MEMS parts onto the substrate. The microparts are fabricated on SOI (silicon-on-insulator) wafers using DRIE (deep-reaction-ion-etching).

As seen in figure 2, automated assembly of the microspectrometer using μ^3 involves: (i) grasping of four MEMS part from the parts die using passive jammer, (ii) maneuvering the parts through collision free paths planned by the path planner, (iii) releasing the parts onto their designated compliant sockets on the device die. Additionally two spherical lenses and one beamsplitter cube are also aligned and assembled on the device die. To ensure high yield we formulate an assemblability criterion and categorize various uncertainties that are associated with microparts and fixtures throughout the microassembly process.

B. High-Yield-Assembly-Condition (HYAC)

Assume that a microassembly process *'P'*, carried out to assemble a specific microsystem. *'P'*, can be further divided into individual subtasks P_1, P_2..., P_n, where *'n'* is the number of continuous operations involving a single robot, a single part or a single tool:

$$P = \sum_{i=1}^{n} P_i \,. \tag{1}$$

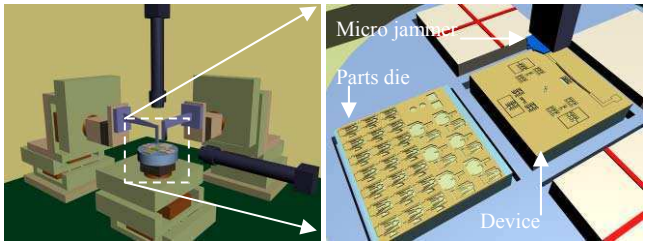

(a) (b)

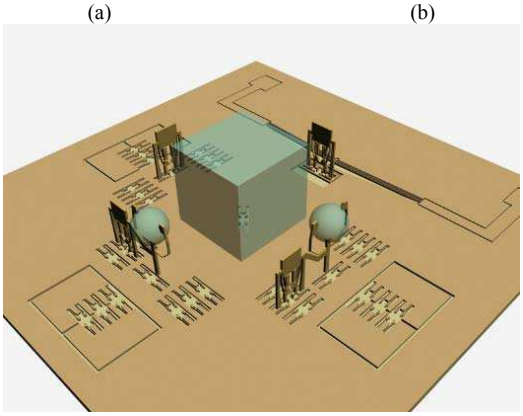

(c)

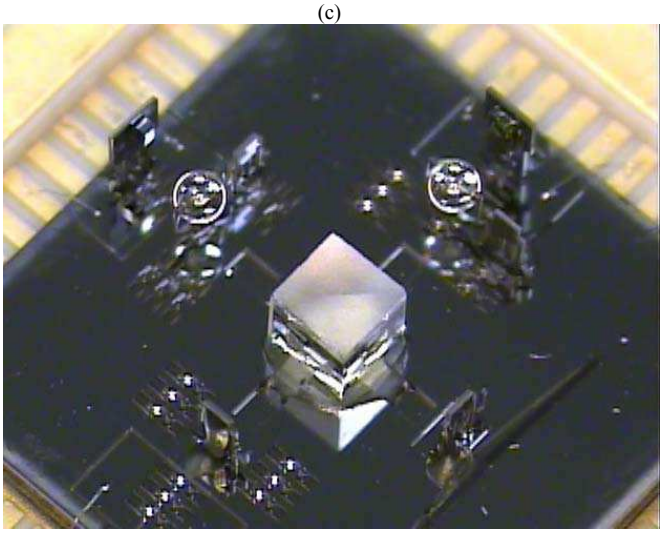

(d)

Figure 2: 3D rendering of assembly configuration of microspectrometer; (a) vitual μ^3 robotic assembly setup (b) close-up view of the micropart (mirrors, grippers, lens holders) and device dies (assembly sockets), (c) diagram of assembled 2½D MEMS parts and off-the-shelf optical components on the spectrometer substrate. (d) Actual microspectrometer assembly [14]

Success of the designated assembly process can be represented as:

$$S(P) = \bigcap_{i=1}^{n} S(P_i) \,, \tag{2}$$

where *'S'* is the success factor of the assembly/bonding process (a Boolean value). From equation (2) it can be inferred that the manufacturing success requires all subtasks to succeed.

We can treat subtasks *'P_i'* as a combination of two types of positioning operations at the microscale: controllable and uncontrollable. Controllable operations *'P_i^m'* refer to spatial manipulation of components using robots. This type of manipulation will be considered to be actively controllable within certain tolerance bounds with Gaussian statistics.

On the other hand, uncontrollable operations *'P_i^b'* refer to change in component position based on the material properties and interaction forces at the microscale. Friction based interference fitting, pneumatic grasping, surface tension, capillary stiction, adhesive bonding etc are some of the examples of uncontrollable operations. They depend on surface properties of the microparts and can act both in favor and against the assembly. We assume such operations to be uncontrollable in the sense that the assembly system will not actively correct their errors. However the effects can be predicted through appropriate models, and can be neglected in certain instances (for instance if passive grippers and snap-fastener connectors are used) [16].

Given a particular assembly task with allowable tolerance distribution σ_1^2, and the error distributions in locating part and robot positioning given as σ_2^2 and σ_3^2 respectively, 99% of yield in assembly can be ensured if:

$$\sigma_1^2 > \sigma_2^2 + \sigma_3^2 \quad . \tag{3}$$

The assembly tolerance distribution σ_1^2 originates from the design of parts and joints as well as errors in fabrication steps. During assembly, parts and fixtures need to be located accurately to deploy the inverse kinematic model for the robotic manipulators. Locating a fixture depends on the workspace identification and sensor precision, errors in which contribute to part error distribution σ_2^2. And finally the robotic links and joints in the manipulator work within a certain accuracy which is affected by motion profile and travel distance. Additionally resolution of a robotic manipulator also factors in correct positioning of the end-effector. Error distributions in these precision parameters of the robotic manipulator jointly constitute the positioning error σ_3^2. There are other factors affecting the yield of microassembly such as dynamics of the robots, effect of contact sensing etc. However, for sufficiently quasi-static conditions for the robots and for non-contact sensors such as vision sensors, we will limit the governing factors for high yield assembly to the above three distributions.

In the High Yield Assembly Condition (HYAC), all error distributions are assumed to be Gaussian, and a step-through description for calculating the variances of equation (3) can be found in [18]. The HYAC is therefore a quantitative way to predict or evaluate the individual success factor *'S'* of assembly. Therefore, in equation (2) $S = 1$ if HYAC is true, and $S = 0$ if HYAC is false for a specific assembly subtask. Furthermore, note that in the inequality for HYAC:

i. *'σ_1^2'* is "measurable" but not "correctable".
ii. *'σ_2^2'* is "measurable" and "correctable" in some cases, but this requires additional sensors or better fixtures.
iii. *'σ_3^2'* is both "measurable" and "correctable"; assuming the robot precision can be improved through control.

In the next sections, the goal of hybrid control will be to satisfy the HYAC and consequently make $S = 1$. A controller will be chosen such that *'σ_3^2'* is minimized, depending on the complexity of the assembly task.

C. Repeatability-Resolution-Accuracy (RRA) rules

The *complexity index (CI) of a subtask*, denoted as *'Ω'*, is defined as a binary value used to classify an assembly subtask as high-yield or low-yield based on associated robot and sensor precisions as well as allowed assembly tolerance budget. A high-yield subtask is executed with faster open loop control, while a low-yield subtask is carried out with more accurate active feedback closed loop control. Denote:

$$\Omega(\sigma_3) = \frac{1 - \mathrm{sgn}(\sigma_2^2 + \sigma_3^2 - \sigma_1^2)}{2}. \tag{4}$$

The precision metrics for the robotic manipulators such as accuracy, repeatability and resolution will determine the values of the complexity index for individual subtasks. First, we slightly redefine conventional precision metrics as follows:

Accuracy: The robotic system is commanded to place the end-effector at a designated position in 3D-space which may involve translation and/or rotation in R^6. A fixed sensor (an optical microscope, in this case) is used to determine the error between actual and desired position of the end-effector. The error distribution with respect to the sensor gives the measure for accuracy, σ_{acc}.

Repeatability: The robotic system has been commanded to place the end-effector alternatively between two predefined but arbitrary points in 3D-space (corresponding to two respective joint coordinate vectors) one of which is measured through a sensor. The error distribution with respect to the sensor gives the measure for repeatbility, σ_{rep}.

Resolution: We define the resolution of the manipulator system as the minimum increment that the manipulator can execute, σ_{res}.

In a hybrid microassembly system, the assembly tasks can be accomplished by a control structure that will be selected among the following cases:

- Controller 1 (open-loop, uncalibrated): A nominal model, robot control using joint sensing only.
- Controller 2 (open-loop, calibrated): A calibrated model, robot control using joint sensing only.
- Controller 3 (closed-loop): Robot control using a heteroceptive sensor and a robot-sensor model.

In [17], we formulated a set of simple decision rules for selecting appropriate controllers that can accomplish microassemblies with a high yield guarantees. The so called Resolution-Repeatability-Accuracy (RRA) rules state that:

1. *Select controller 1 only when* $\Omega(\sigma_{acc}) = 1$..
2. *Select controller 2 only when* $\Omega(\sigma_{rep}) = 1$.
3. *Select controller 3 only when* $\Omega(\sigma_{res}) = 1$.

III. Hybrid Control for Microassembly

The complexity index *'Ω'* is used for control loop selection during execution. The hybrid control diagram is shown in figure 3. The state space model shown in figure 5 is a modified version of standard output feedback control system. In the modified model the feedback *'K'* is selectable through the complexity index *'Ω'* by introducing it as an input along with *'r(n)'*, which is the "precision-adjusted" path-planning input.

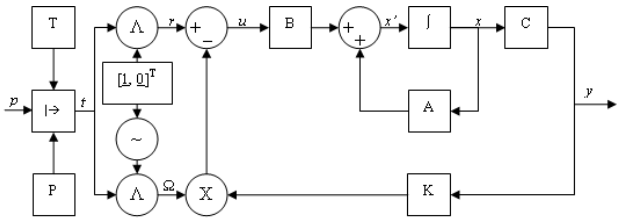

Figure 3: Precision adjusted hybrid controller for microassembly

The new input to the system is represented as;

$$t[n] = [r[n] \quad \Omega[n]]^T, \tag{15}$$

where *'Ω'* is the complexity index. The simplified discrete state space model is given as follows:

$$\begin{aligned} x[n+1] &= (A - B(\Omega[n]K)C)x[n] + Br[n] \\ y[n] &= Cx[n] \end{aligned} \tag{16}$$

In equation (16) Ω = 0 reduces the control to open loop and Ω = 1 selects the closed loop control.

The precision adjusted hybrid controller has been implemented in real time for microspectrometer assembly and some of the experimental results are shown in this section. First, we examined for cycle time in the microassembly. Two cases are considered;

i. Open-loop control case, using 3-point calibration, in which the cycle time is the sum of [calibration time] & [distance/speed of robot].
ii. Closed-loop control case using a visual servoing scheme in which the cycle time is the sum of [Jacobian identification time] & [servo time].

The in open-loop, the cruising speed of the robot was kept uniform at 1mm/s which would take, on an average, 40s to 50s to pick up a MEMS part from the parts die and assemble it on the device die (as shown in figure 2) through pure open loop control. If we add the time for calibration, which takes around 50 to 60 seconds, the open loop controlled assembly can be done within 90 to 100 seconds which is reasonably good.

However, in actuality, open loop control does not provide enough accuracy for longer/complex paths and alignments with tight tolerances. We examined for the efficiency of the hybrid controller in terms of overall accuracy and process time, as shown in figure 4. The motion has been executed using (i) open loop – calibrated control, (ii) closed loop control and (iii) proposed hybrid controller. As seen in figure 4, for 10 actual assembly attempts of micromirrors using each of the three control structures, the hybrid controller gives 35% better accuracy than the open loop controller, while its throughput is 60% faster than a closed-loop controller.

Typical value for the assembly tolerance *'σ_1'* was 3.3µm. 6 out of 10 assembly attempts failed in the open loop case, where as the hybrid control managed to achieve a higher accuracy and thus succeeded in assembling all 10 microparts. Closed loop control also succeeded in assembling all 10 parts however it took a much longer long time (2.5 slower).

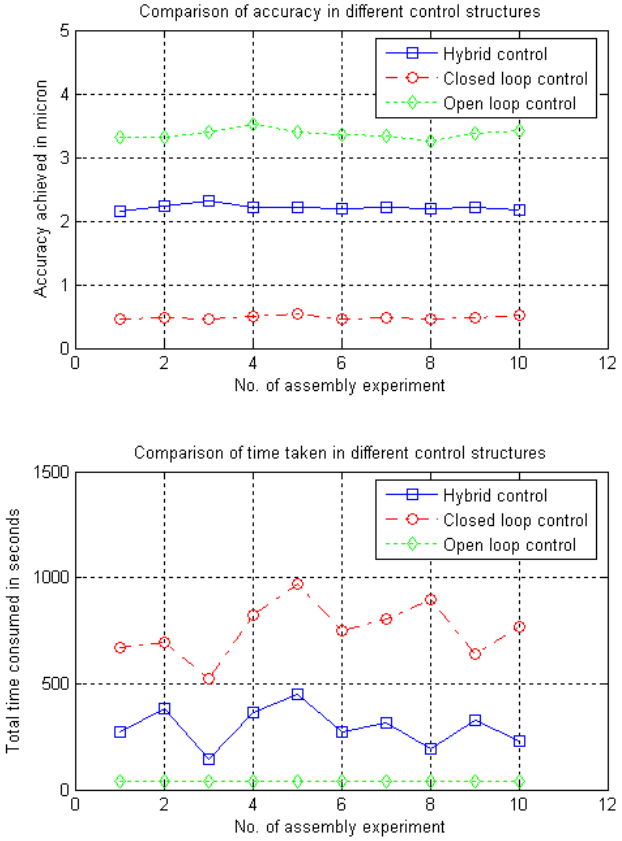

Figure 4: Comparative analysis of precision adjusted hybrid controller with open loop and closed loop control (results from 10 microassembly attempts in each case are shown)

IV. Conclusion and Future Work

Manufacturing of microsystems can be approached either through monolithic fabrication methods or through microassembly. Although stochastic microassembly can theoretically achieve much larger throughputs within small time in comparison to serial deterministic assembly, it is difficult to use it to construct complex, 3D devices. On the other hand, serial microassembly can, but it requires careful tuning to improve the assembly yield and throughput

simultaneously. In this paper, we propose a precision adjusted hybrid controller in order to improve the yield and speed of microassembly. The assembly complexity is used to dynamically select an open or closed loop control mode via a hybrid controller. Several experiments conducted for the assembly of a microspectrometer, show that the hybrid control provides 35% more accuracy than open loop control, while the throughput is 60% higher than closed loop control.

Future work include further characterization and refinement of the controller, including formal performance guarantees, and a study of tradeoffs between real-time change in tolerances, cycle time and yield, and dynamic reconfiguration of the system for other microassembly tasks.

.

REFERENCES

[1] Y. Zhou, B.J. Nelson, and B. Vikramaditya, "Fusing force and vision feedback for micromanipulation," in Proceedings Of IEEE International Conference on Robotics and Automation, Leuven, Belgium, May 1998.

[2] A. M. Hoover, S. Avadhanula, R. Groff, Ronald S. Fearing, "A Rapidly Prototyped 2-Axis Positioning Stage for Microassembly Using Large Displacement Compliant Mechanisms" in Proceedings of IEEE International Conference on Robotics and Automation, Orlando, Florida, May 2006.

[3] D.O.Popa, H.Stephanou, "Micro and meso scale robotic assembly", in SME Journal of Manufacturing Processes, Vol. 6, No.1, pp. 52-71, 2004.

[4] A. Rizzi, J. Gowdy, R.L. Hollis, "Agile assembly architecture: an agent based approach to modular precision assembly systems," in Proceedings of IEEE International Conference on Robotics and Automation, Volume: 2, pp. 1511 – 1516, April 1997.

[5] Cohn M. B, Böhringer K. F et al, "Microassembly technologies for MEMS", International Society for Optical Engineering Proceedings, vol. 3513, pp. 2-16.

[6] Dechev .N, Cleghorn .W.L.; Mills .J.K, "Microassembly of 3-D microstructures using a compliant, passive microgripper", Journal of Microelectromechanical Systems, Volume 13, Issue 2, pp. 176-189, April 2004.

[7] M. Shimada, J. A. Tompson, J. Yan, R. J. Wood, and R. S. Fearing, "Prototyping millirobots using dextrous microassembly and folding," in Proceedings of ASME IMECE/DSCD, vol.69-2, pp.933-940, 2000.

[8] F. Arai, T. Fukuda, "Adhesion-type micron-endeffector for micromanipulation," in Proceedings of IEEE International Conference on Robotics and Automation, pp.1472-1477, 1997.

[9] K. F. Bohringer, et. al., "Sensorless manipulation using massively parallel microfabricated actuator arrays," in Proceedings of IEEE International Conference on Robotics and Automation, pp.826-833, 1998.

[10] G. Gatti, D. Mundo, G.Danieli, "A combined feedforward and feedback control strategy to improve the dynamic performance of cam-follower systems", 12th IFToMM World Congress, Besançon (France), June 2007.

[11] D. Ruiz-Vega, M. Glavic, D. Ernst, "Transient Stability Emergency Control Combining Open-Loop and Closed-Loop Techniques", In Proceedings of the IEEE PES 2003 Summer Meeting. Toronto, Canada, July 2003.

[12] P. De Man, A. Preumont, "Hybrid feedback-feedforward control for vibration suppression", Journal of Structural Control, vol.3, No. 1-2, June 1996.

[13] Q. Zhou, P. Kallio, H.N. Koivo, "Model-based Handling and Planning in Micro Assembly," 2nd International Workshop on Microfactories (IWMF) Fribourg, Switzerland, pp. 71-74, October 2000.

[14] A. N. Das, J. Sin, D. O. Popa, H. E. Stephanou, "On the Precision Alignment and Hybrid Assembly Aspects in Manufacturing of a Microspectrometer," Proceedings of IEEE Conference on Automation Science and Engineering (CASE), Washington DC, USA, August 2008.

[15] A.N.Das, P.Zhang, W.H.Lee, D.O.Popa, and H.E.Stephanou, "μ^3: Multiscale, deterministic micro-nano assembly system for construction of on-wafer micro-robots," in Proceedings of IEEE International Conference on Robotics and Automation (ICRA 07), vol. 10, no. 14, Rome, Italy, pp. 461–466, April 2007.

[16] R. Murthy, A.N. Das, D.O. Popa, "High Yield Assembly of Compliant MEMS Snap Fasteners," Proceedings of the ASME 2008 International Design Engineering Technical Conferences & Computers and Information in Engineering Conference, Brooklyn, New York, USA.

[17] D.O. Popa, R. Murthy, A. N. Das, "M3- Deterministic, Multiscale, Multirobot Platform for Microsystems Packaging: Design and Quasi-Static Precision Evaluation," to appear in IEEE Transactions on Automation Science and Engineering (T-ASE), 2009.

[18] D.O. Popa, "High Yield Automated MEMS Assembly," to appear in Robotic Microassembly, ed. M. Gauthier, S. Reigner, Willey, 2009.

Towards the mechanical and control-oriented optimization of micromechatronic systems for robust control

Mathieu Grossard, Nicolas Chaillet, Mehdi Boukallel, Arnaud Hubert and Christine Rotinat-Libersa

***Abstract*— This work presents a new method developed for the optimal design of piezoactive compliant micromechanisms. It is based on a flexible building block method, called FlexIn, which uses an evolutionary approach, to optimize a truss-like planar structure made of passive and active building blocks, made of piezoelectric material. An electromechanical approach, based on a mixed finite element formulation, is used to establish the model of the active piezoelectric blocks. From the first design step, in addition to conventional mechanical criteria, innovative control-based metrics can be considered in the optimization procedure to fit the open-loop frequency response of the synthesized mechanisms. In particular, these criteria have been drawn here to optimize modal controllability and observability of the system, which is particularly interesting when considering control of flexible structures. Then, a planar monolithic compliant micro-actuator has been synthesized using FlexIn and prototyped. Finally, simulations and experimental tests of the FlexIn optimally synthetized device demonstrate the interests of the proposed optimization method for the design of micro-actuators, microrobots, and more generally for adaptronic structures.**

***Index Terms*— Actuator design, balanced gramian, compliant mechanisms, controllability, microgripper, microrobotics, observability, piezoelectricity, topology optimization, vibrations control.**

I. INTRODUCTION

IN many applications including Micro Electro Mechanical Systems (MEMS) [1], [2], [3], [53] smart structures [4], [5], [54] surgical tools [6], [7], etc, compliant mechanisms have already been used. They are single-body, elastic continua flexible structures, that deliver the desired motion by undergoing elastic deformation, as opposed to jointed rigid body motions of conventional mechanisms. When considering small scale systems (e.g. for microrobotics use), there are many advantages of compliant mechanisms.

To improve such active compliant micromechanisms performances, it can be useful to optimize them from the first designing step, taking into account versatile microrobotic criteria [19] . A global systematic design approach is presented in this paper, where topology optimization of the piezoactive structure, as well as that of its frequency response, is used to design compliant smart mechanisms. This method is based on the flexible building block method called FlexIn ("Flexible Innovation"). It considers a planar compliant mechanism as an assembly of both passive and piezoactive compliant building blocks, and uses a multi-objective genetic algorithm to optimize these structures. To complete the panel of purely mechanical criteria, innovative control-based metrics have been newly proposed in FlexIn. These criteria are useful tools to ensure the efficient control of the flexible structures afterwards.

Firstly, we will briefly review the underlying idea of the FlexIn methodology for the optimal design of smart compliant mechanisms.Secondly, a topology design strategy is drawn to take into account, in the optimization algorithm, accurate model-reduction and control of flexible structures. In addition to purely static mechanical criteria, two new control-oriented metrics are simultaneously used to optimally synthesize a compliant piezoactuator.

Manuscript received February 20th, 2009.

M. Grossard, M. Boukallel and C. Rotinat-Libersa are with the CEA LIST, Interactive Robotics Unit, Fontenay-aux-Roses, F-92265 France. mathieu.grossard@cea.fr

N. Chaillet and A. Hubert are with the FEMTO-ST Inst., UMR CNRS 6174 - UFC / ENSMM / UTBM, Automatic Control and Micro-Mechatronic Systems depart. (AS2M department), 25000 Besancon - France. nicolas.chaillet@ens2m.fr

II. FLEXIN: A COMPLIANT MECHANISM STOCHASTIC DESIGN METHODOLOGY

We briefly present the flexible building block method, which has been implemented for the optimal design of micromechanical planar mechanisms in a software called FlexIn (developed with $Matlab^{®}$). It uses a multi-objective evolutionary algorithm approach for the optimal design of smart compliant mechanisms made of an assembly of elementary passive and active compliant building blocks, chosen in two specific libraries. Detailed descriptions of the method can also be found in [27], [28], [29], [30], [31].

A. Compliant building blocks

Two libraries of compliant elements in limited number are proposed in FlexIn. These bases are composed respectively of 36 passive and 19 piezoactive block elements, made of beams assembly (Fig.1). They are sufficient to build a high variety of topologies.

B. Principles of the method and design parameters

The purpose of FlexIn is to optimally design realistic compliant structures. The specification of a planar compliant mechanism problem considers specific boundary conditions: fixed frame location, input (actuators), contacts and output (end-effector). Different types of actuation principles can be used: either external or internal force/displacement actuators defined at particular nodes of the mesh [28], or integrated piezoactive elements taken from the active library above [29], [31]. The design method consists of searching for an optimal distribution of allowed passive and active building blocks,

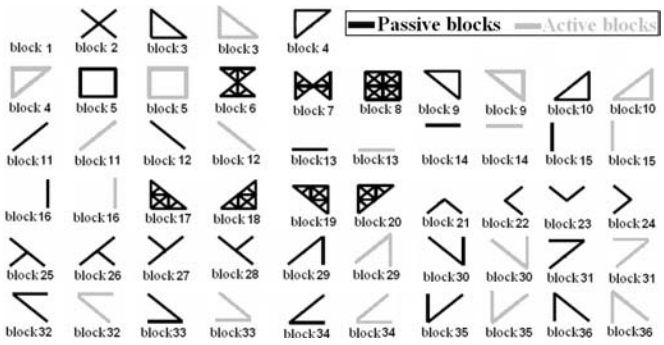

Fig. 1. Passive (black) and piezoactive (grey) libraries of compliant building blocks, for planar compliant mechanisms synthesis using FlexIn.

as well as for the optimal set of structural parameters and materials, in order to obtain relevant monolithic compliant structures. The location of fixed nodes, contacts, and that of the actuators and/or piezoactuated blocks can also be considered as optimization parameters.

C. Multi-criteria genetic algorithm

Many fitness functions are available in FlexIn, thus allowing the optimal synthesis of devices within a wide schedule of conditions.

- Several static mechanical fitness can be specified for the optimization problem: free displacement and blocking force at the output port, geometric advantage (GA) i.e. ratio between output and input strokes, mechanical advantage (MA) i.e. ratio between output and input forces, etc.
- Various dynamic control-oriented metrics have been newly implemented in FlexIn to meet specific control requirements for microrobotics devices [26]. Obviously, the design strategy depends on the metrics chosen, which must be based on the real needs for the device use.

D. Electro-mechanical FE model of the piezoelectric structures

1) Elementary piezoelectric beam: In FlexIn, it is assumed that the compliant mechanisms are undergoing structural deformations, mainly due to the in-plane bending of the beams constituting the blocks. Thus, the models of the blocks are obtained considering Navier-Bernoulli beam type finite elements. Structural parameters of each rectangular block are height, width and thickness. Material characteristics of each block are parameterized by Young's modulus, Poisson's ratio, yield strength, density, and piezoelectric coefficients for the piezoactive blocks. To allow the calculation of different optimization criteria, FlexIn uses the FE model of each block of the libraries. To obtain the FE formulation of the piezoelectric blocks, a model of a piezoelectric beam is first needed. We consider that the piezoceramic beams constituting the blocks are perfectly bonded to electrodes at their lower and upper faces (Fig.2). Exploiting the transverse effect of piezoelectricity, longitudinal deformation S_{11} along L dimension is generated under the transverse electric field E_3.

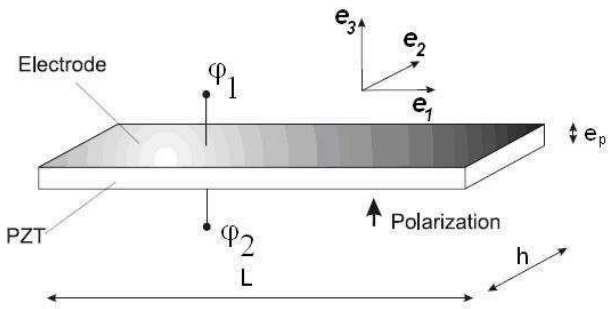

Fig. 2. Thickness-polarized piezoelectric beam transducer with electroded surfaces, and orientation in the material reference frame $(\mathbf{e_1}, \mathbf{e_2}, \mathbf{e_3})$. φ_1 and φ_2 denotes the electric potential of the electrodes.

2) Calculation of the active block FE model matrices: The active blocks present some various topologies, as shown in (Fig.1). Their advantage is that they can furnish multiple coupled degrees of freedom (dofs), thus generating more complex movements with only one building block. The mass, stiffness and electromechanical coupling matrices of each piezoactuated block are obtained by the assembly of mass, stiffness and electromechanical coupling matrices of beams, which are expressed in the global coordinate system.

3) FE model of piezoeletric structures: The mass, stiffness and electromechanical coupling matrices of each block are calculated numerically, considering every combination of the discrete values allowed for the structural optimization variables, i.e. material and size of the blocks. Thus, the calculation of the different matrices of each valued-block is done one time only at the beginning of the optimal design problem (before running the genetic algorithm), which saves running time.

During the optimization, candidate structures are generated by the genetic algorithm. The conservative dynamic behaviour of a structure is described through its mass, stiffness and electromechanical coupling matrices, obtained by the assembly of the matrices of all the blocks constituting the structure. This assembly is done during the optimisation process at each generation and for each individual.

III. Useful measures for evaluation of input-output transfer performances of flexible systems

A. New criteria for control-oriented design of compliant structures with FlexIn

The two significant design tasks in flexible structure control are the identification of the dominant modes to build an appropriate reduced model, and the control strategy design.

1) Reduced model: Since the dynamic model of a flexible structure is characterized by a large number of resonant modes, accurate identification of all the dominant system

dynamics often leads to very high order model. Thus, a model reduction is required.

In FlexIn, a first criterion has been drawn to optimize the reduced-model accuracy of the systems, while limiting spillover effects. Given a set of structures to optimize, the optimal structures are chosen as the ones guaranteeing the highest joint controllability and observability for all the modes in the bandwidth of interest, while providing the minimum joint controllability and observability of the neglected modes (Fig.3). This criterion will enable the rise of structures with accurate reduced model, based on a few highly dominant modes, allowing the easy identification and computation of state model.

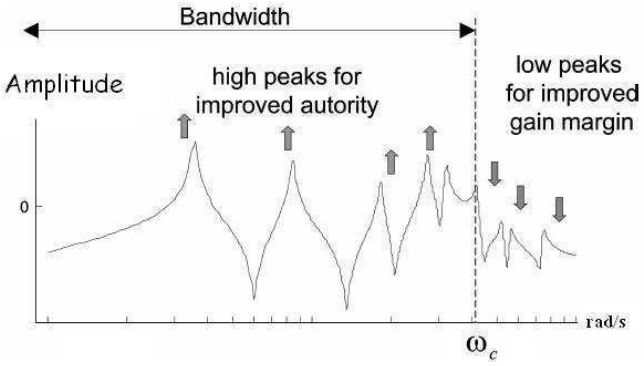

Fig. 3. Desired form of the open-loop FRF.

2) A pseudo-collocated active structure: There are a number of difficulties associated with the control of flexible structures (amongst them, variable resonance frequencies and highly resonant dynamics).

For some specific class of flexible structures, which can be modeled as collocated resonant systems, active damping controllers (PPF, IFF,...) have proven to offer greater robustness, performance, and ease of implementation relatively to traditional techniques. They are often focused on damping the dominant modes [40]. Although the flexible structures rarely present natural collocated designs, an other optimization criterion, based on the modal expansion of $SISO$ systems transfer function, has been established in FlexIn to force the structures to have an actuator/sensor collocated behaviour in terms of frequency response function (Fig.4).

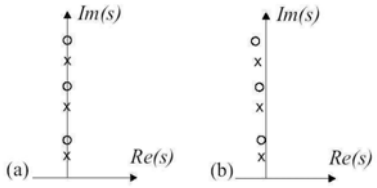

Fig. 4. Poles (x) and zeros (o) locations of a collocated system: (a) undamped, (b) lightly damped (Figure is symmetric towards Real axis).

These two new criteria, when used simultaneously, provide a great deal of information concerning the closed-loop device performances that are achievable with this particular open-loop frequency configurations. In FlexIn, an evaluation function was implemented to be used in the optimization process in order to obtain systems designs with collocated type open-loop transfer function, forcing the resonances (poles) and antiresonances (zeros) alternating in the reduced model. Inspired by [40] and [46], these criteria concern all the modes contained in the frequency spectrum of the first k dominant modes, where the alternative is desired. (In our application case k is set to 2.)

B. Multiobjective optimal synthesis of a monolithic compliant piezoactuator

The concepts presented previously have been applied to the design of a microgripper actuator, considering a multicriteria optimization problem, with both static mechanical (stroke and force at the output node of the structure) and the two new control-oriented fitnesses.

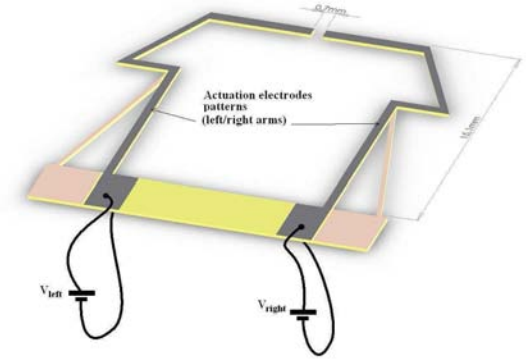

Fig. 5. $3D$ CAD model of the piezoeletric device with top face electrode patterns. V_{left} (resp. V_{right}) is the controlled input for actuating the left (resp. right) arm.

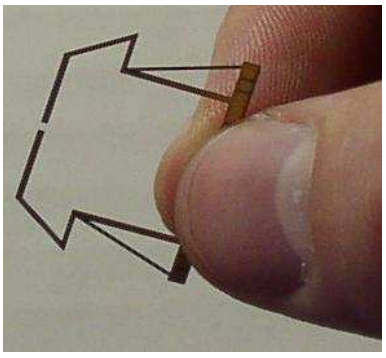

Fig. 6. Photo of the prototyped piezoelectric monolithic device, obtained by laser cutting and made of a single piezoelectric material PIC151 from PI Piezo Ceramic Technology [48]

From the set of pseudo-optimal solutions generated by FlexIn, one solution, whose topology is presented on Fig.5 and Fig.6, is studied here in more details. Actually, active blocks are those which will be bonded with electrodes, exploiting the inverse piezoelectric effect, while passive

blocks will be made in the same piezoelectric material but without electrodes. When actuated under $\pm 100V$, the gripper produces high stroke $\delta_x = \pm 10.69 \mu m$ and blocking force $F_x = 0.84N$ at the fingertip. Morevover, its frequency response function shape is the one intended (Fig.7) : the authority control on the two first resonant modes is more important than the following modes, and alternating pole/zero pattern is preserved in that spectrum of interest.

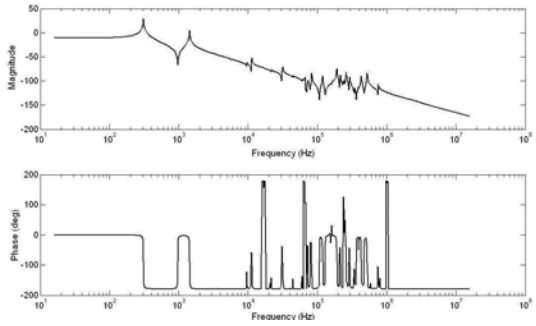

Fig. 7. Bode diagram of the structure between input (voltage u, in V) and output (deflexion δ_x, in μm) simulated by FlexIn.

IV. Conclusions

A new concept of optimal design method for smart compliant mechanisms has been presented. This method, called FlexIn, can consider a smart compliant mechanism as an assembly of passive and active compliant building blocks made of PZT, so that actuators are really integrated in the structure.

Complex multi-objective design problems can be solved by FlexIn, taking advantage of versatile criteria to synthesize high performance microrobotic flexible mechanisms designs. In addition to classical mechanical criteria, currently encountered in topology optimization (i.e. force and displacement maximization), FlexIn considers now simultaneously efficient control-based criteria.

References

[1] Lee W.H., Kang B.H., Oh Y.S., Stephanou H., Sanderson A.C., Skidmore G., Ellis M., "Micropeg manipulation with a compliant microgripper", in Proc. IEEE Int. Conf. on Robotics and Automation, Taipei, Taiwan, pp. 3213-3218, September 2003.

[2] Chang H.C., Tsai J.M.L., Tsai H.C., Fang W., "Design, fabrication, and testing of a 3-DOF HARM micromanipulator on (111) silicon substrate", Sensors and Actuators, vol. 125, pp. 438-445, 2006.

[3] Kota S., Ananthasuresh G.K., Crary S.B., and Wise K. D., "Design and fabrication of micro-electromechanical systems", ASME Journal of Mechanical Design, vol. 116, pp. 1081-1088, 1994.

[4] Saggere L., Kota S., "Static shape control of smart structures using compliant mechanisms", AIAA Journal, vol. 37, pp. 572-578, 1999.

[5] Kim D.H., Lee M.G., Kim B., Sun Y., "A superelastic alloy microgripper with embedded electromagnetic actuators and piezoelectric force sensors: a numerical and experimental study", Smart Materials and Structures, vol. 14, pp.1265-1272, 2005.

[6] Frecker M., Haluck R., "Design of a multifunctional compliant instrument for minimally invasive surgery", Journal of Biomedical Engineering, vol. 127, pp. 990-993, November 2005.

[7] Houston K., Sieber A., Eder C., Tonet O., Menciassi A., Dario P., "Novel Haptic Tool and Input Device for Real Time Bilateral Biomanipulation addressing Endoscopic Surgery ", Proc. of the 29th Annual International Conference of the IEEE EMBS, Lyon, France, August 23-26, pp. 198-201, 2007.

[8] Breguet J.M., and al., "Monolithic piezoceramic flexible structure for micromanipulation", 9th International Precision Engineering Seminar and 4th International Conference on Ultraprecision in Manufacturing Engineering, pp. 397-400, Braunschweig Germany, 1997.

[9] Agnus J., Nectoux P. , Chaillet N., "Overview of microgrippers and micromanipulation station based on a MMOC microgripper", Proc. of the IEEE International Symposium on Computational Intelligence in Robotics and Automation, pp. 117-123, 2005.

[10] Frecker M., Canfield S., "Optimal design and experimental validation of compliant mechanical amplifiers for piezoceramic stack actuators", Journal of Intelligent Material Systems and Structures, vol. 11, pp. 360-369, 2000.

[11] Kota S., "Tailoring unconventional actuators using compliant transmissions : design methods and applications", IEEE/ASME Transactions on Mechatronics, vol. 4, pp. 396-408, December 1999.

[12] Lau G. K., and al., "Systematic design of displacement - amplifying mechanisms for piezoelectric stacked actuators using topology optimization", Journal of Intelligent Material Systems and Structures, vol. 3985, pp. 583-591, 2000.

[13] Barboni R., and al., "Optimal placement of PZT actuators for the control of beam dynamics", Smart Material and Structures, pp. 110-120, 2000.

[14] Maddisetty H., Frecker M., "Dynamic topology optimization of compliant mechanisms and piezoceramic actuators", ASME Journal of Mechanical Design, vol. 126, pp. 975-983, 2002.

[15] Abdalla M., and al., "Design of a piezoelectric actuator and compliant mechanism combination for maximum energy efficiency", Smart Material and Structures, vol. 14, pp. 1421-1430, 2005.

[16] Nelli Silva E.C., Kikuchi N., "Design of piezoelectric transducers using topology optimization", Smart Material and Structures, vol. 8, pp. 350 -365, USA, 1999.

[17] Fablbusch S., and al., "Flexible Microrobotic System MINIMAN: Design, Actuation Principle and control", Proc. of the IEEE/ASME International Conference on Advanced Intelligent Mechatronics, pp. 156-161, Atlanta, Georgia USA, 1999.

[18] Du H., and al., "Topological optimization of mechanical amplifiers for piezoelectric actuators under dynamic motion", Smart Material and Structures, vol. 9, pp. 788-800, 2000.

[19] Frecker M., "Recent advances in optimization of smart structures and actuators", Journal of Intelligent Material Systems and Structures, vol.14, pp. 207-216, April/May 2003.

[20] Jonckheere E. A., "Principal components analysis of flexible systems - Open-loop case", IEEE Trans. on Automatic Control, vol. 29, pp. 1095-1097, 1984.

[21] Kermani M. R., Moallem M., Patel R. V., "Optimizing the performance of piezoelectric actuators for active vibration control", in Proc. of IEEE International Conference on Robotics and Automation, Washington DC, pp. 2375-2380, 2002.

[22] Chen W., and al., "Optimal sensor design and control of piezoelectric laminate beams", IEEE Trans. on Control Systems and Technology, vol. 12, pp. 148-155, 2004.

[23] Collet M., "Shape optimization of piezoelectric sensors dealing with spill-over instability", IEEE Trans. on Control Systems Technology, vol. 9, pp. 654-662, 2001.

[24] Kermani M. R., Patel R. V., Moallem M., "Flexure control using piezostack actuators: design and implementation", IEEE/ASME Trans. on Mechatronics, vol. 10, pp. 181-188, 2005.

[25] Liu W., Hou Z., Demetriou M. A., "A computational scheme for the optimal sensor/actuator placement of flexible structures using spatial H2 measures", Mechanical Systems and Signal Processing, vol. 20, pp. 881-895, 2006.

[26] Grossard M., Rotinat-Libersa C., Chaillet N., "Gramian-based optimal design of a dynamic stroke amplifier compliant micro-mechanism", IEEE/RSJ International Conference on Robots and Systems, San Diego, USA, 2007.

[27] Bernardoni P., and al., "A new compliant mechanism design methodology based on flexible building blocks", Smart Material and Structures, vol. 5383, pp. 244-254, USA, 2004.

[28] Bernardoni P., "Outils et méthodes de conception de structures mécaniques à déformations réparties et actionnement discret - applications en microrobotique" , PhD Thesis realized at the CEA, University Paris 6, France, 2004.

[29] Grossard M., Rotinat-Libersa C., Chaillet N., "Redesign of the MMOC microgripper piezoactuator using a new topological method",

IEEE/ASME International Conference on Advanced Intelligent Mechatronics, Zürich, Switzerland, 2007.

[30] Rotinat-Libersa C., Perrot Y., Friconneau J.-P., "Potentialities of optimal design methods and associated numerical tools for the development of new micro- and nano- intelligent systems based on structural compliance - An example -", IARP- IEEE/RAS-EURON JointWorkshop on Micro and Nano Robotics, Paris, France, 2006.

[31] Grossard M., Rotinat-Libersa C., Chaillet N., Perrot Y., "Flexible building blocks method for the optimal design of compliant mechanisms using piezoelectric material", 12th IFToMM World Congress, Besançon, France, 2007.

[32] Deb K., and al., "A fast elitist non-dominated sorting genetic algothm for multi-objective optimization: Nsga-II", Proc. of the 6th International Conference on Parallel Problem Solving from Nature, pp. 849-858, France, 2000.

[33] ANSI/IEEE Std. 176-1987 IEEE Standard on piezoelectricity, 1987.

[34] Hagood N. W., Chung W. H., Von Flotow A., "Modelling of piezoelectric actuator dynamics for active structural control", Journal of Intelligent Material Systems and Structures, vol. 1, pp. 327-354, 1990.

[35] Preumont A., "Mechatronics: Dynamics of Electromechanical and Piezoelectric Systems (Solid Mechanics and its Applications)", published by Springer, September, 2006.

[36] Moore B.C., "Principal component analysis in linear systems: controllability, observability, and model reduction", IEEE Transactions on Automatic Control, vol. 26, 1981.

[37] Abreu G. L. C., Ribeiro M., Steffen J. F., "Experiments on optimal vibration control of a flexible beam containing piezoelectric sensors and actuators", Journal of Shock and Vibration, vol. 10, pp. 283-300, 2003.

[38] Halim D., Moheimani S. O. R., "Experimental implementation of spatial H_∞ control on a piezoelectric laminate beam", IEEE/ASME Transactions on Mechatronics, vol. 4, pp. 346-356, 2002.

[39] Halim D., Moheimani S. O. R., "Spatial H_2 control of a piezoelectric laminate beam: experimental implementation", IEEE Transactions on Control System Technology, vol. 10, pp. 533-546, 2002.

[40] Aphale S. S., Fleming A.J., Moheimani S. O. R., "Integral resonant control of collocated smart structures", Smart Materials and Structures, vol.16, pp. 439-446, 2007.

[41] Lim K. B., Gawronski W., "Actuators and sensor placement for control of flexible structures", in Control and Dynamics Systems: Advances in Theory and Applications, ed. London, Academic Press, 1993.

[42] Hac A., Liu L., "Sensor and actuator location in motion control of flexible structures", Journal of Sound and Vibrations, vol. 167, pp. 239-261, 1993.

[43] Gawronski W., Lim K. B., "Balanced control of Flexible structures", Springer, London, 1996.

[44] Glover K., "All optimal Hankel-norm approximations of linear multivariable systems and their L^∞-error bounds", International Journal of Control, vol. 39, pp. 1115-1193, 1984.

[45] Gevarter W. B., "Basic relations for control of flexible vehicles", AIAA Journal, vol. 8, pp. 666-672, 1970.

[46] Martin G. D., "On the control of flexible mechanical systems", PhD Dissertation, Stanford University, USA, 1978.

[47] Fanson J. L., Caughey T. K., "Positive position feedback-control for large space structures", AIAA Journal, vol. 28, pp. 717-724, 1990.

[48] PI Piezo Ceramic Technology, Available: http://www.piceramic.com/, 2005.

[49] Main J. A., Garcia E., Newton D. V., "Precision position control of piezoelectric actuators using charge feedback", Journal of guidance, Control and Dynamics, vol. 18, pp. 1068-1073, 1995.

[50] Ge P., Jouaneh M., "Generalised preisach model for hysteresis nonlinearity of piezoelectric actuators", Precision Engineering, vol. 20, pp. 99-111, 1997.

[51] Den Hamer A. J., Angelis G. Z., Roozen N. B., "Broad-band active vibration suppression using PPF focused on industrial applications", IEEE/ASME Transactions on Mechatronics, vol. 10, pp. 146-153, 2005.

[52] Putra A. S., Sunan H., Kok K. T., Panda S. K., Tong H. L., "Self-sensing actuation with adaptive control in applications with switching trajectory", IEEE/ASME Transactions on Mechatronics, vol. 13, pp. 104-111, 2008.

[53] Fatikow S., Wich T., Hulsen H., Sievers T., Jahnisch M., "Microrobot system for automatic nanohandling inside a scanning electron microscope", IEEE/ASME Transactions on Mechatronics, vol. 12, pp. 244-252, 2007.

[54] Basset P., Kaiser A., Legrand B., Collard D., Buchaillot L., "Complete system for wireless powering and remote control of electrostatic actuators by inductive coupling", IEEE/ASME Transactions on Mechatronics, vol. 12, pp. 23-31, 2007.

Robust Vision-Guided Multi-probe Microassembly

John Wason and John T. Wen
Center for Automation Technologies & Systems (CATS)
Rensselaer Polytechnic Institute
Troy, NY 12180

***Abstract*— In this workshop presentation, we will present the control algorithm development and experimental results for the 3D assembly of sub-millimeter parts using multiple sharp probes and vision feedback. Current approaches to microassembly emulates macroassembly strategies by using micro-grippers to handle parts and sometimes force sensors to guide insertion. However, grippers and force sensors are fragile. The ability to manipulate parts is further constrained by the limited range of motion of micro-robotic manipulators. We will show that the probe based approach is more robust and versatile to handle micro-parts. With vision feedback, repeatable and reliable 3D part manipulation has been achieved. Our experimental testbed consists of two 6-DOF actuated probes, an actuated die stage, and vision feedback. The kinematic relationships for the probes, die stage, and part manipulation are calibrated for kinematics-based planning and control. The effect of adhesion forces on probe-part and part-stage contacts is investigated in order to achieve grasp stability and robust part manipulation. Vision routines are developed to allow features to be located in three dimensional space through stereo vision. By combining pre-planned manipulation sequences and vision-based manipulation, repeatable spatial (in contrast to planar) manipulation and insertion of a sub-millimeter part has been shown.**

I. Introduction

Modern silicon fabrication technologies have provided the ability to create electro-mechanical devices at the micro-scale using techniques originally designed for the fabrication of integrated circuits. While the understanding of the behavior of these devices has advanced significantly, a reliable method for assembling parts still does not exist [1]. Currently, most devices are designed to be monolithic, and do not require assembly. This approach has made significant advances, but the resulting monolithic devices are severely limited in functionality when compared to spatial devices that have been assembled from multiple parts. This research investigates the possibility of spatial microassembly using multiple sharp probes instead of using grippers or other exotic methods such as probabilistic assembly or electric force fields. The initial problem posed was to simply insert a small (sub-millimeter) part into a slot. The part needs to be lifted, rotated out of plane, and inserted. Figure 1 shows a photo of the part before it is picked up and after it has been inserted. This simple task is intended to be a first step toward assembling complex spatial structures involving multiple parts.

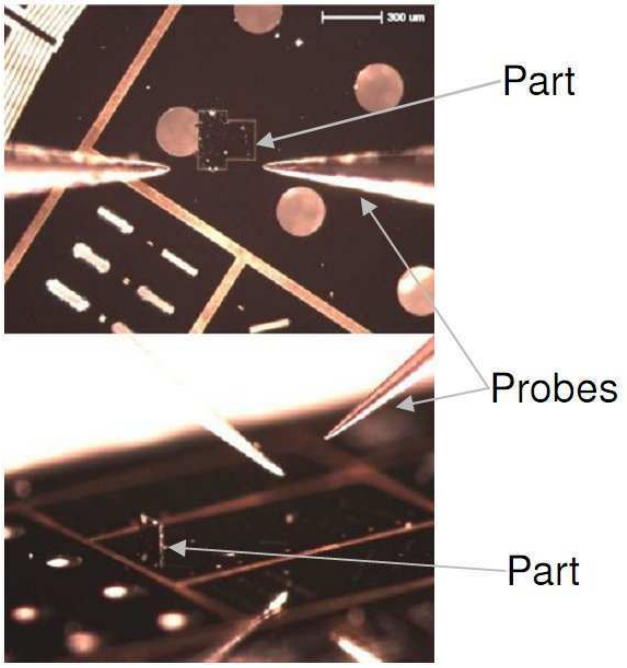

Fig. 1. NIST Part Before and After Insertion

Previous work on microassembly has primarily focused on the use of micro-grippers. Unfortunately, the parts being handled adhered to the manipulators even after they were opened. This is because the physical effects that are important on the macro scale, such as friction, gravity, and inertia, become insignificant on the micro scale compared to a set of adhesion forces. These forces are thought to consist of electrostatic attraction, Van der Waals force, and fluidic forces [2]. Micro-grippers also demonstrated poor performance due to their fragility. They are made out of exotic materials such as bimorph metals or piezoelectric ceramics [2], or are silicon MEMS devices themselves [3]. Contact force and alignment have to be tightly controlled, or the manipulator can be damaged. These two main issues have limited the adoption of micro-gripper based assembly techniques.

Several examples of microassembly techniques not utilizing micro-grippers have been investigated. These techniques include electrostatic fields [4], chop-stick like microhands

John Wason is a Ph.D. candidate in the Dept. of Mechanical, Nuclear, & Aerospace Engineering, Rensselaer Polytechnic Institute, wasonj@rpi.edu
John Wen is the Director of the CATS, Rensselaer Polytechnic Institute, wenj@rpi.edu

[5], random self assembly [6], and simple contact manipulators that include probes and flat surfaces [7], [8]. These manipulation strategies attempt to overcome the inherent difficulty of using MEMS actuators to achieve part manipulation. The assembly method described in this paper belongs to the simple contact class of manipulation techniques. Two actuated sharp-tip (10 μm diameter) probes and a stationary probe are used to achieve spatial assembly of MEMS parts.

The overall goal of our research is to demonstrate the feasibility of using the proposed 3-probe system to produce a flexible and robust microassembly workcell. Because of the inherent limitations on fabrication and design techniques of MEMS devices, the resulting technique will need to be tolerant of deviations of the source materials and errors that occur during the assembly itself. The resulting system will also have to capable of being quickly adapted to different assembly tasks; design iteration and evolution occurs rapidly in the fast paced production environment of microfabrication. The single part insertion task described in this talk is intended to be a first iteration proof of concept that part handling with sharp-tip probes is an effective means to satisfy these goals.

II. Vision

The primary means of feedback for our microassembly system is image processing based machine vision. The vision feedback system is based on two high-resolution feedback camera augmented with stepper motors to provide automated zoom capabilities. One camera is configured as an overhead camera, while another camera provides a side view approximately 20 degrees off horizontal. The two cameras are calibrated to each other by perturbing the die and locating reference marks. By using the two cameras it is possible to locate a 3D point anywhere in the workspace.

The use of vision feedback instead of other sensing technologies used in previous work has many advantages. The primary advantages of vision sensing are robustness, the richness of information, low cost, and lack of hysteresis. Vision systems are robust in that they are easily handled. Other sensors have shown to be extremely fragile – even a minute amount of force can cause damage to or destruction of the device. Vision sensing provides a complete view of the workspace and has the potential to provide extensive information on the state of the system. The cameras in use on the system are low cost but provide resolution below a micron. Finally, there is no hysteresis in the vision system. Force sensors tend to have a large amount of hysteresis, or can be affected by motion.

Feature detection of items on the die has not been straightforward due to the scale of the items being identified. Small dust particles tend to collect on the surface and have a wide statistical variation. The dust is unavoidable, as breaking the parts free from the tethers generates debris that adheres to the surfaces. This debris triggers standard feature detectors, reducing their effectiveness. Instead, a template matching scheme is employed that is based on the direct convolution method that is often used in this type of problem. Templates are initialized from knowledge of the shape of the item being tracked and are rotated and convoluted to determine the best match. The convolution is done through the use of Fast Fourier Transform, and rotation is accomplished by regenerating the template from the template definition information.

III. Insertion Process

The single part microinsertion task considered in this research is intended to be an iterative step toward multiple part microassembly. A silicon part measuring $300\times300\times25$ micrometers is shaped to fit vertically into a slot as shown in Figure 1. The microassembly system needs to grasp and lift the part off of a flat surface on which the part is lying and then rotate it out of plane to the vertical position. Once rotated, the part is aligned with a slot and inserted. An automated insertion process has been developed utilizing vision feedback. The part is initially placed on the die surface manually by the operator. The rest of the insertion process including part location, grasping, manipulation, insertion, and release are all fully automated. The manipulation has shown to be very robust. With the current system an entire insertion process takes around 8 minutes, but this can be reduced by the use of faster cameras and image processing software. Figure 2 shows snapshots of the insertion process.

Acknowledgment

This work is also supported in part by the Center for Automation Technologies and Systems (CATS) under a block grant from the New York State Foundation for Science, Technology and Innovation (NYSTAR), and in part by the National Science Foundation (NSF) Smart Lighting Engineering Research Center (EEC-0812056).

References

[1] Quan Zhou, Pasi Kallio, and Heikki N. Koivo. Modeling of micro operations for virtual micromanipulation. In *SPIE Conference on Microrobotics and Microassembly*, volume 3834, Boston, MA, 1999.

[2] Y. Zhou and B. J. Nelson. The effect of material properties and gripping force on micrograsping. In *Proceedings of the 2000 IEEE Conference on Robotics & Automation*, San Francisco, CA, April 2000.

[3] D.O. Popa, B. H. Kang, J.T. Wen, H. E. Stephanou, G. Skidmore, and A. Geisberger. Dynamic modeling and input shaping of thermal bimorph mems actuators. In *IEEE International Conference on Robotics and Automation*, Taipei, Taiwan, 3002.

[4] K. Bohringer, K. Goldberg, M. Cohn, R. Howe, and A Pisano. Parallel microassembly with electrostatic force fields. In *International Conference on Robotics & Automation*, Leuven, Belgium, May 1998.

[5] T. Tanikawa and T. Arai. Development of a micro-manipulation system having a two-fingered micro-hand. *IEEE Transactions on Robotics and Automation*, (1), February 1999.

[6] E. Saeedi, S. S. Kim, J. R. Etzkorn, , D. R. Meldrum, and B. A. Parviz. Automation and yield of micron-scale self-assembly process. In *Third ANnual IEEE Conference on Automation Science and Engineering*, Scottsdale, AZ, 2007.

[7] J. J. Gorman and N. G. Dagalakis. Probe-based micro-scale manipulation and assembly using force feedback. In *International Conference on Robotics and Remote Systems for Hazardous Environments*, pages 621–628, Salt Lake City, UT, 2006.

[8] A. Ferreira, C. Cassier, and S. Hirai. Automatic microassembly system assisted by vison servoing and virtual reality. *IEEE/ASME Transactions on Mechatronics*, 9(2):321–333, June 2004.

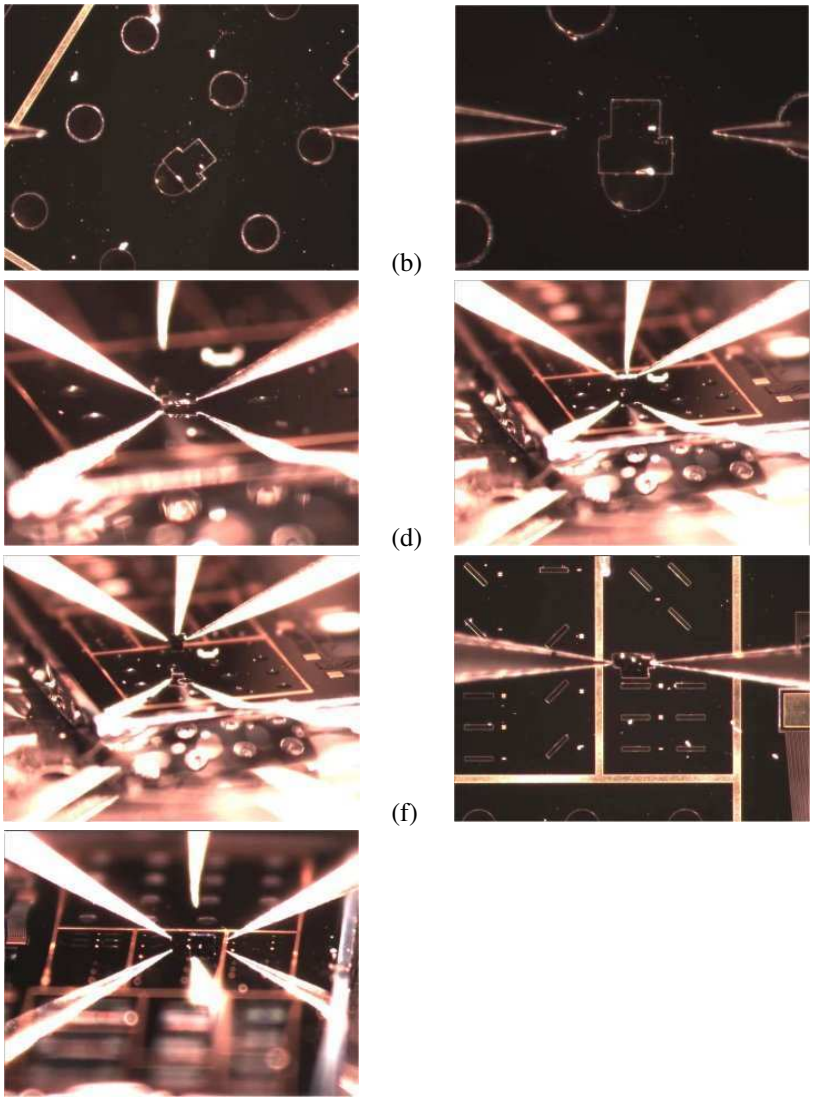

Fig. 2. (a) Initial Part Position (b) Part rotated and probes moved close to part (c) Probes gripping part after automated sequence (d) Part at start of out of plane rotation (e) Part after out of plane rotation (f) Part and slot pre-aligned (g) Part inserted

Fast and Precise Micropipette Positioning System based on Continuous Camera-Robot Recalibration and Visual Servoing

Leonardo S. Mattos and Darwin G. Caldwell
Italian Institute of Technology

***Abstract*— Micro-biomanipulations rely on fine motion control and precise tool positioning for the execution of delicate operations on biological structures. Appropriate control is typically enabled by the use of micromanipulators; however, manual execution of biomanipulations is difficult, requiring extensive operator training (up to 1 year) and meticulous work under fatiguing conditions. Automation can be an alternative to improve such operations. In this case, challenges such as interface design, system integration, acquisition of feedback data, and the design of control systems have to be dealt with. Here we address a new strategy to deal with the later problem, proposing the creation of a fast and precise pipette positioning system based on continuous recalibration of mapping functions and visual servoing. Trials show this system effectively eliminates precision problems related to tool position drifts and robot speed limitations imposed by vision systems.**

EXTENDED ABSTRACT

MICRO-biomanipulation typically deals with the positioning, injection and delivery of foreign material into microscopic and very delicate biological structures, such as cells and early embryos. These structures often have dimensions smaller than 100μm, although large variations exist between different cell types or different kinds of embryos. Nevertheless, the standard biomanipulation tools are glass pipettes with fine tips, which are attached to microinjectors that provide precise fluid control. Due to the very small size and transparency of biological structures, biomanipulations are performed under inverted microscopes with special optics and high magnifications (e.g. up to 400x). In addition, tool positioning is controlled through micromanipulators, which are mechanical/electro-mechanical devices that scale down the operator's commands, offering control resolution compatible with the structures being manipulated.

The common characteristic between different biomanipulation operations is that they all require very precise pipette positioning and high motion resolution. These can be achieved manually using modern micromanipulators; however, the operations are still difficult, requiring meticulous control, long biomanipulation sessions and extensive operator training, e.g., typically 2-hours long microinjection sessions and up to one year of training for the case of embryo microinjections [1].

L. Mattos is with the Italian Institute of Technology, Via Morego 30, 16163 Genova, Italy (phone: +39-010-71781409; fax: +39-010-720321; e-mail: leonardo.demattos@iit.it).

D. Caldwell is with the Italian Institute of Technology, Via Morego 30, 16163 Genova, Italy (e-mail: darwin.caldwell@iit.it).

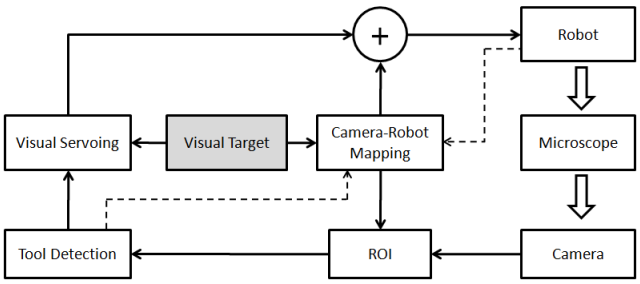

Fig. 1. Block diagram of the micropipette positioning system.

Therefore, robotics may provide a solution to increase the speed, consistency and efficiency of the operations. At the same time, robotic techniques can reduce the training time for new operators. For example, experiments with a teleoperated system developed for the injection of stem cells into early mice embryos have shown that previously untrained operators were able within three microinjection sessions (6 hours) to achieved success rates comparable to that attained by experienced manual microinjection operators [2].

Process automation can offer further benefits. Automation can produce fast biomanipulation systems, enabling batch operations with high-throughput, high consistency and high efficiency [3]. In addition, automated systems can nowadays be built from high-end commercial equipment, including high-precision motorized micromanipulators and motorized microscopes, which are generally flexible and applicable to a number of different operations [4]. However, challenges have to be overcome before actually implementing a successful automated biomanipulation system.

The first challenge for automation in this area consists of the design and development of interfaces for the integration and control of the biomanipulation equipment [5]. Then, there is the need to obtain feedback information for automatic control, which calls for a robust vision system capable of recognizing the biological structures and the micromanipulation tools [6][7][8]. Finally, there is the problem of actually controlling the biomanipulation system using the obtained feedback. This has traditionally been solved through visual servoing systems [7][9][10] or through the definition of mapping functions from the image space to the task space [11][12][13]. Here we concentrate in this later problem, i.e., in creating a new strategy for fast and precise control of the micromanipulation robot.

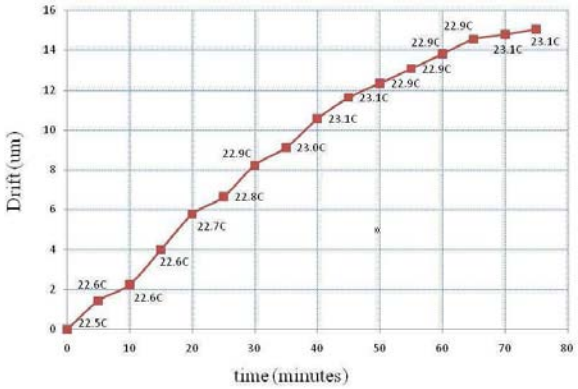

Fig. 2. Tool position drift observed during 75 minutes. The micromanipulator was turned off during this experiment and the data labels show the room temperature in Celsius.

Visual servoing enables very precise tool positioning with sub-pixel resolution in image space. However, it is totally dependent on image processing algorithms, which should provide the motion controller with the coordinates of tools and targets. Errors in the localization algorithms can produce erroneous (and potentially disastrous) robot motion commands, so they should be minimized. This is a difficult task due to noise and occlusions observed in a typical biomanipulation scenario. In addition, the processing of high-definition video images is computationally expensive, so small search windows are used to speed up the computations. This "trick" can result in limitations on the maximum allowable robot speed, which may be kept low to ensure the tool does not leave the search window between consecutive video frames. Maximum robot speed may also be limited to allow for proper imaging of the tool since fast motions cause its image to become blurred. Therefore, our first goal in this research was to augment a traditional visual servoing system to enable fast motions, while maintaining its positioning precision and the robustness of the image processing algorithms.

The use of mapping functions between coordinate frames is another method that can be used to automate biomanipulations. In this case, target coordinates defined in image space are transformed into task-space coordinates, which are then used for "blind" control of the micromanipulation tool. This method does not suffer from processing limitations, but it requires meticulous calibration of the camera-robot system [13][14] or the experimental definition of a look-up table relating both coordinate frames [12]. However, drifts in tool position can affect even the most precise calibration or look-up table. These may be caused by temperature variations, mechanical vibrations, or by step miscounting on encoderless joints driven by stepper motors. For example, our system suffered from tool position drifts, as Fig. 2 shows. Hence, the second goal of this research was to develop a strategy to compensate for the effect of drifts in the system and enable fast "blind" robot positioning based on the camera-robot mapping functions.

The proposed strategy for creating a fast and precise pipette positioning system consisted of combining the two techniques described above, as shown in Fig. 1. In our system, fast motions were achieved through camera-robot mapping, and precise positioning was realized by visual servoing. This effectively eliminated the robot speed limitations imposed by the image processing system while maintaining the precision and robustness of the visual servoing system.

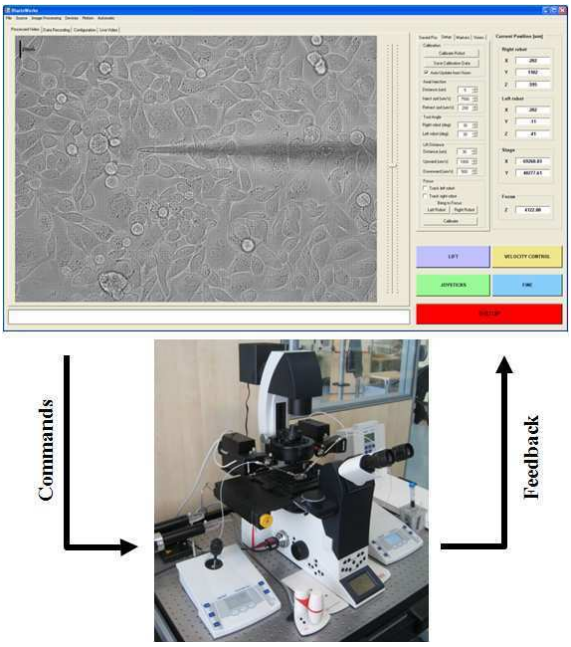

Fig. 3. Control program interface and the biomanipulation setup.

The micromanipulation system used in this research was a conventional biomanipulation setup similar to those currently in use at many neuroscience research laboratories. It included an inverted microscope (Leica DMI6000B), a high-definition video camera (AVT Guppy F-080C), two motorized micromanipulators (Eppendorf TransferMan NK2) and a desktop computer for remote control of all system devices. A picture of the system is shown in Fig. 3 and more details about its configuration can be found in [4].

Here, the camera-robot mapping was initially estimated through a quick and simple calibration procedure, which involved requesting the user to click on the tool tip seen on the live video for five different robot locations. Computation time was kept low by assuming zero image distortion by the system optics and perfect parallelism between the camera plane and the robot's X-Y plane. Therefore, the mapping was approximated to a coordinate transformation between 2-D spaces, simplifying the determination of the translations, rotations and scaling factors required to map points between the two frames. The average positioning error resulting from the use of this mapping was measured to be 5.65µm over 300 targets defined in a 400µm x 300µm area. In this case the maximum robot speed was set to its peak value, i.e. 7500µm/s, and the achieved positioning speed was 48 targets/minute.

In addition to enabling very fast positioning, the camera-

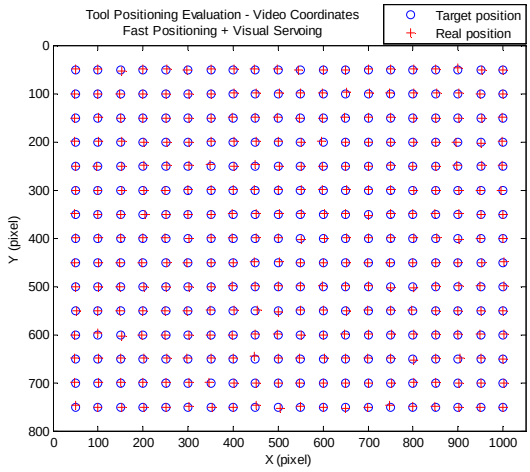

Fig. 4. Evaluation of the final system's tool positioning precision. Measurements were based on 300 targets defined within a 400µm x 300µm area. In this case, the system precision was set to ±2 pixels on both X and Y axes and the resulting average positioning error was 2.02 pixels (0.81µm).

robot calibration was also used for defining a small search window for tool localizations on the video images. In this case, robot coordinates obtained from the controller where mapped to the image space and used as the center point of the tool search window. This new strategy helped to speed-up tool localizations by limiting the pipette search to a guaranteed region of interest (gROI). It also eliminated gross localization errors due to noise or false matches on other objects in the images, thus increasing the robustness of the vision system.

The implemented tool localization algorithm was based on cross-correlation template matching. Its output was used as the feedback information for a visual servoing system, which provided precise tool positioning using a PID (proportional-integral-derivative) control loop. This controller was tuned for stable operation throughout the entire field of view of the camera, presenting a 2.6s rise time, 3.2s settling time, and a maximum observed over-shoot of 2.4%. Experiments with this tuned controller demonstrated an average positioning speed of 8.4 targets/minute.

Visual servoing evaluation experiments over the same 300 targets defined within a 400µm x 300µm area resulted in an overall average positioning error of 0.84µm. This error was within the expected range for the given precision setting, which considered the target reached when the position errors on both X and Y axes were less than 2 pixels (or 0.8µm for the specific magnification used during the trials). Additionally, this very small error makes the positioning system appropriate to the manipulation of cells with dimensions down to 10µm.

Another use of the tool localization information gathered from the vision system relates to solving the tool drift problem observed in our system. In this case, tool coordinates in image space (acquired from the vision system) were paired to tool coordinates in task space (acquired directly from the robot controller) to build up new calibration data points. These points were then used for continuous online recalibration of the camera-robot mapping parameters, which effectively eliminated the impact of tool drift on the mapping precision.

The final system achieved its goals and realized fast and precise pipette positioning by combining the use of camera-robot mapping, continuous mapping recalibration, and visual servoing. System evaluation demonstrated an average positioning speed of 13.4 targets/minute and an average positioning error of 0.81µm over the same 300 test targets previously used (see Fig. 4). These results show that the developed system was successful in making good use of the fast motion capabilities of the micromanipulation robot while maintaining the precision of visual servoing techniques.

REFERENCES

[1] D. Kim, S. Yun, B. Kim, and S. Kwon, "Mechanical force response of single living cells using a microrobotic system," *Proceedings of the 2004 IEEE ICRA*, New Orleans, USA, April 2004.

[2] L. Mattos, E. Grant, R. Thresher, and K. Kluckman, "Improving blastocyst microinjections through teleoperation," *IEEE Transactions on Information Technology in Biomedicine*, submitted for publication.

[3] W. H. Wang, X. Y. Liu, and Y. Sun, "Hi*gh-Throughput Automated Injection of Individual Biological* Cells," *IEEE Transactions on Automation Science and Engineering*, accepted for future publication.

[4] L. Mattos and D. Caldwell, "Interface Design for MicroBiomanipulation and Teleoperation," *Proceedings of the Second International Conference on Advances in Computer-Human Interactions*, ACHI 2009, Mexico, February 2009.

[5] A. Bzostek, R. Kumar, N. Hata, O. Schorr, R. Kikinis, R. Taylor, "Distributed Modular Computer-Integrated Robotic Systems," *Proceedings of the Third International Conference on Medical Image Computing and Computer-Assisted Intervention*, pp. 969-978, 2000.

[6] K. Sakaki, N. Dechev, E. J. Park, R. D. Burke, "Development of a five degree-of-freedom biomanipulator for autonomous single cell electroporation," *Proceedings of the 2007 IEEE/RSJ International Conference on Intelligent Robots and Systems*, San Diego, USA, October 2007.

[7] Y. Sun and B. Nelson, "Biological cell injection using an autonomous microrobotic system," *The International Journal of Robotics Research* (IJRR), Vol.21, pp. 861-868, 2002.

[8] H.M. Wang and J.Y. Zhu, "A Precise Visual Control Method for Micromanipulator," *CIRP Annals - Manufacturing Technology*, vol. 53, issue 1, 2004, pp. 17–20.

[9] W. Zhao, W. Zhang, M. Gupta, G. Zong, and P. Ouyang, "A micro visual servo system for biological cell manipulation: Overview and new developments," *Seventh International Conference on Control, Automation, Robotics and Vision*, pp. 429-434, Singapore, December 2002.

[10] L. Mattos, E. Grant, R. Thresher, K. Kluckman, "From Teleoperated to Automatic Blastocyst Microinjections: Designing a New System from Expert-Controlled Operations," *Proceedings of the 2008 IEEE/RSJ International Conference on Intelligent Robots and Systems*, Nice, France, September 2008.

[11] M. Sitti and H. Hashimoto, "Two-Dimensional Fine Particle Positioning Under Optical Microscope Using a Piezoresistive Cantilever as a Manipulator", *Journal of Micromechatronics*, vol. 1, issue 1, 2000, pp. 25–48.

[12] C. Pawashe and M. Sitti, "Two-dimensional vision-based autonomous microparticle manipulation using a nanoprobe," *Journal of Micromechatronics*, vol. 3, n. 3–4, 2006, pp. 285–306.

[13] M. Ammi, V. Fremont, A. Ferreira, "Flexible microscope calibration using virtual pattern for 3-D telemicromanipulation," *Proceedings of the 2005 IEEE International Conference on Robotics and Automation*, Barcelona, Spain, April 2005.

[14] Y. Zhou and B. J. Nelson, "Calibration of a parametric model of an optical microscope", *Optical Engineering*, December 1999, pp. 1989-1995.

Control of an Active Handheld Instrument for Microsurgery and Micromanipulation

Robert A. MacLachlan, *Member, IEEE,* Brian C. Becker, *Student Member, IEEE* and Cameron N. Riviere, *Member, IEEE*

Abstract—"Micron" is a fully handheld manipulator that enhances accuracy in microsurgery and micromanipulation by active compensation of the physiological hand tremor of the user. To sense the motion of the device in six degrees of freedom, a set of four LEDs is tracked by orthogonally placed planar photodiodes. Three LEDs are affixed to the tip manipulator, and the fourth is mounted on the tool handle, which is also the base of the manipulator. The LEDs are pulsed at different rates, and a frequency-domain multiplexing scheme is used to track each light source separately with roughly micron precision at 2000-Hz sampling. The sensory information is used to enable feedback control of the tip manipulator, which is a 3-dof parallel mechanism driven by Thunder® piezoelectric actuators to provide accuracy enhancement in a workspace approximately 0.6 mm x 3 mm x 3 mm.

I. Introduction

RECENT years have seen several approaches to improvement of accuracy during retinal microsurgery, including telerobotic systems [1, 2] and the steady-hand approach [3, 4]. This paper presents a description of the control system of "Micron," an active handheld manipulator designed to enhance accuracy in microsurgery and other micromanipulation by compensation of the hand tremor of the user.

II. System Description

The major system components of Micron are the handpiece/manipulator combination, custom driver and signal conditioning electronics, two position-sensitive detector (PSD) "cameras," and a PC with data acquisition cards and Labview real-time control software. Optical measurement determines the six-degree-of-freedom pose of the handgrip and tool. A feedback loop running at 2 kilosamples/sec servos the tool tip to a computed goal position.

The Micron concept has demanding position measurement requirements because low-latency, high-resolution position feedback is required for closed-loop control of the high-bandwidth manipulator. The position measurement subsystem optically tracks the pose of the tool and hand grip at 2 kHz with micron resolution over a 4-cm workspace, using two PSDs, signal conditioning electronics, infrared light-emitting diodes (IR LEDs) and LED driver, a data acquisition card, and signal processing software.

A PSD is a specialized large-area photodiode that makes an analog position measurement of the centroid of a light source. A lens focuses the IR light onto the PSD. A long-pass IR filter excludes much ambient light, reducing interference and shot noise. We refer to this lens/filter/PSD combination as a camera, though it does not capture an image. Each camera allows measurement of LED position in two degrees of freedom. Each PSD measures multiple LED positions simultaneously using frequency domain multiplexing [5]. The LEDs are modulated at distinct frequencies between 8 kHz and 20 kHz.

Two separate PSD cameras allow each light position to be triangulated in three dimensions. The tool pose is recovered from the positions of a triad of LEDs mounted on the tool holder. The handle pose is reconstructed from the tool pose using only one additional LED mounted on the handle. This can be done because the manipulator has only three degrees of freedom.

The piezoelectric actuators require high voltage (-240 V to 480 V) but minimal current (1 mA peak). They are driven by a custom bidirectional current source. Driving by current rather than voltage has two advantages: linearity and safety. It has long been known [6] that hysteresis and nonlinearity in piezoelectric actuators can be greatly reduced by controlling the total charge stored in the actuator rather than the applied voltage. Charge control schemes must provide some way to keep the output voltage from drifting in the inevitable presence of leakage currents and other errors. In Micron this is achieved by a voltage feedback loop that estimates the current error by slowly servoing the voltage drift to zero.

The current handpiece houses the manipulator and LEDs in a 50-mm diameter housing mounted on the front end of the handgrip (Fig. 1). Although the present prototype is bulkier than desired, the indented star-like shape of the housing allows the tool to be held within 15 mm of the microscope sightline without obstructing the operator's view. The grip itself contains only wiring. The LEDs are visible through windows in the housing.

Manuscript received February 25, 2009. This work was supported in part by the U.S. National Institutes of Health under Grants R01 EB007969 and R21 EY016359, and by the American Society for Laser Medicine and Surgery.

R. A. MacLachlan is with the Robotics Institute, Carnegie Mellon University, Pittsburgh, PA 15213 USA (e-mail: ram@cs.cmu.edu).

B. C. Becker is with the Robotics Institute, Carnegie Mellon University, Pittsburgh, PA 15213 USA (e-mail: brianbec@andrew.cmu.edu).

C. N. Riviere is with the Robotics Institute, Carnegie Mellon University, Pittsburgh, PA 15213 USA (phone: 412-268-3083; fax: 412-268-7350; e-mail: camr@ri.cmu.edu).

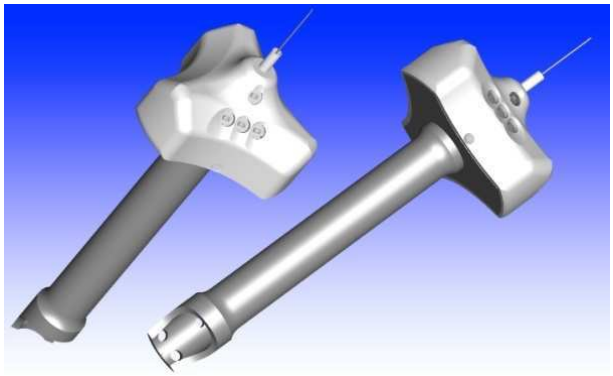

Fig. 1. Two views of the exterior housing of Micron, showing the handgrip and the three-pointed star-shaped manipulator, with the four LEDs that are used for optical tracking.

The manipulator has a 3DOF parallel configuration. The requirements for the manipulator include high bandwidth, accuracy to several microns, close to 1 mm axial range of motion, 2-3 mm transverse range of motion, and compactness sufficient to fit within a handheld tool. An important enabling technology for the present prototype is a unique piezoelectric bender actuator (Thunder TH-10R, Face Technologies) that uses a laminated metal construction to give a range of motion exceeding that of all-ceramic bender (bimorph) actuators while generating newtons of force and having a stiffness consistent with high control bandwidth. Each leg of the manipulator consists of two actuators mechanically connected in series in a face-to-face folded configuration. Due to the actuator kinematics, this generates approximately 600 microns of motion, which is three times the range of motion of a single actuator. Each actuator assembly is rigidly fixed to the base plate and connected to the star-shaped output plate by a polypropylene monofilament flexure. The flexure allows free motion of the actuators and output plate, absorbing both bend and shear displacements.

A flex-circuit is used to make the connections between the cable and the electrical components. A clear bore through the handgrip and manipulator allows end-effector leads such as wires, tubes, and optical fibers to pass through the handle.

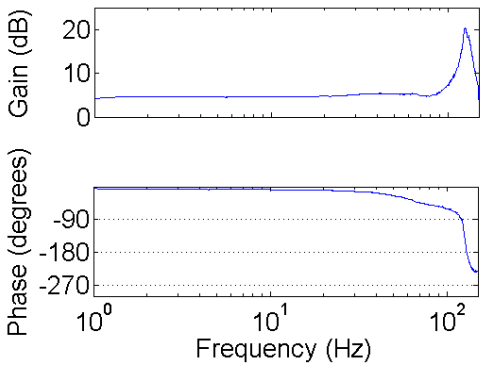

Fig. 2. Frequency response of the manipulator.

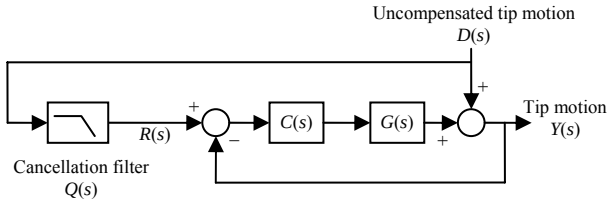

Fig. 3. Small-signal model including cancellation filter.

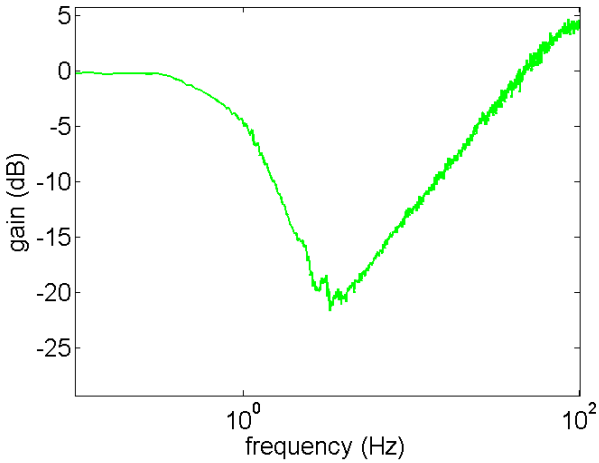

Fig. 4. Frequency response of Micron active handheld accuracy enhancement system.

The manipulator's response, $G(s)$, is relatively flat at low frequencies, and is dominated by a resonance at 174 Hz (Fig. 2). With the present PID controller it is necessary to set the loop bandwidth well below the resonance so that there is adequate gain margin at the resonance. Although small amounts of derivative gain help to stabilize the system at the resonance, the system dynamics at and below the system bandwidth (52 Hz) are dominated by the integral gain.

In the Micron active error compensation scenario, the manipulator generates a motion which, added to the hand tremor, $D(s)$, comprises the overall tip motion, $Y(s)$. The controller, $C(s)$, compensate for the manipulator dynamics, $G(s)$, in order to drive the tip to the desired position, $R(s)$.

To generate the desired position for tremor suppression, a low-pass filter is used, leading to the small-signal model depicted in Fig. 3. Micron thus exhibits a band-stop response (Fig. 4); of necessity, gain is unity at low frequency, as the tip follows gross handle motion, and reverts again to unity at high frequency, due to finite cancellation bandwidth. The position of the low corner of the stop-band is set by the cancellation filter, $Q(s)$, according to a tradeoff between tremor suppression and response time. The high corner is set by the loop bandwidth, which is (as noted above) determined by the highest integral gain consistent with stability, set by the control algorithm and the dynamics of the manipulator. This high corner is not desirable, and pushing it to higher frequency is a goal of future development.

A consideration for the use of the system is that the frequency response is being introduced into the operator's

eye-hand feedback loop, so the low frequency part of the response affects the operator's subjective "feel." If the response is too fast or poorly damped, it may feel twitchy or bouncy.

The handle light position is used to generate the position in world coordinates of the center of the workspace. Because this is where the tip would be in a conventional rigid tool this point is used as the nominal tip position, which is then passed through the cancellation filter to give the compensated goal position in world coordinates.

Although the true inverse kinematics is nonlinear, due to the small angular deflection, a linear approximation works well. The link lengths are set as commanded by the controller output; then, on the next cycle, the resulting actual position is again read by the optical tracker, closing the feedback loop. This feedback minimizes all of the effects that disturb the tip from the desired goal position: hand tremor, inexact inverse kinematics, and contact forces encountered by the manipulator.

The controller operates in the manipulator space, primarily so that it can recover gracefully when the manipulator saturates due to reaching the limit of its travel. Manipulator saturation due to large rapid hand motion is a significant problem in handheld experiments. Firstly, it prevents error cancellation; secondly, it opens the feedback loop, revealing undesirable dynamics, especially integrator windup in the controller, $C(s)$. This problem is a subject of current research in the project.

III. Results

Fig. 5 shows an example of the tremor suppression performance of the system, comparing compensated and uncompensated the measured frequency response of the ASAP-micron system. In this case the user was attempting to hold the tool motionless, so any tip motion is undesirable.

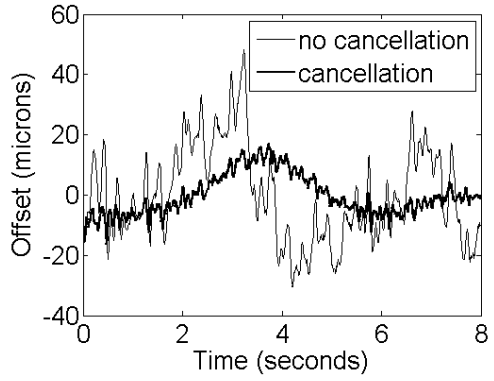

Fig. 5. A sample of recorded hand tremor, both with and without compensation. The tremor was played back through a P-611 NanoCube™ nanopositioner (Polytec PI) in place of the user's hand, to allow repeated testing.

References

[1] I. W. Hunter, T. D. Doukoglou, S. R. Lafontaine, P. G. Charette, L. A. Jones, M. A. Sagar, G. D. Mallinson, and P. J. Hunter, "A teleoperated microsurgical robot and associated virtual environment for eye surgery," *Presence*, vol. 2, pp. 265-280, 1993.

[2] H. Das, H. Zak, J. Johnson, J. Crouch, and D. Frambach, "Evaluation of a telerobotic system to assist surgeons in microsurgery," *Comput. Aided Surg.*, vol. 4, pp. 15-25, 1999.

[3] R. Taylor, P. Jensen, L. Whitcomb, A. Barnes, R. Kumar, D. Stoianovici, P. Gupta, Z. Wang, J. de Juan, E, and L. Kavoussi, "A steady-hand robotic system for microsurgical augmentation," *Int. J. Rob. Res.*, vol. 18, pp. 1201-1210, 1999.

[4] B. Mitchell, J. Koo, I. Iordachita, P. Kazanzides, A. Kapoor, J. Handa, G. Hager, and R. Taylor, "Development and application of a new steady-hand manipulator for retinal surgery," in *Proc. IEEE Int. Conf. Robot. Autom.*, 2007, pp. 623-629.

[5] R. A. MacLachlan and C. N. Riviere, "High-speed microscale optical tracking using digital frequency-domain multiplexing," *IEEE Trans. Instrum. Meas.*, in press.

[6] C. Newcomb and I. Flinn, "Improving the linearity of piezoelectric ceramic actuators," *Electron. Lett.*, vol. 18, pp. 442-444, 1982.